

utions The Newsletter for Vol 3: 2011 Cell Biology Researchers

Profiling Cellular Energy

Multiplexed Quantification of Oxidative Phosphorylation Parameters as a Mechanistic Indicator for Drug-Induced Mitochondrial Toxicity Page 3

Functional Human Oligodendrocyte Progenitors Provide Optimized *In Vitro* Differentiation for Studies of Myelinization Page 6

Fast and Gentle Enrichment Assays for Isolating and Staining Native Protein-Cytoskeleton Associations Page 11

ESGRO®-2i Medium: Inhibitor-Based Serum-free Medium for ES and iPS Cell Culture Page 17

A Dual Platform Approach to Cytokine Analysis of Effector CD4+ T-Cells Page 21

Rapid Counting of Somatic Cells in Dairy Milk Using the Scepter™ 2.0 Cell Counter, Following Spin-Wash Sample Preparation Page 25

Exciting New Products for Cell Biology Research

To subscribe to the quarterly Cellutions newsletter, please visit www.millipore.com/cellquarterlynews





Versatility in a Complete Package.

MILLIPLEX® MAP magnetic bead-based immunoassay kits & MAGPIX® instruments.



Research can change direction in a minute—to keep the pace, you need a versatile assay platform.

With our analytically validated MILLIPLEX® MAP kits, using Luminex® xMAP® technology, measure one analyte per sample or fifty, in research areas including neuroscience, toxicity, oncology, cellular metabolism—using preconfigured or customized panels.

And, the versatility doesn't stop there—we're the original multiplex partner offering the full range of Luminex® instruments, including MAGPIX®, the newest, most flexible, small-footprint instrument for the user-friendly xMAP® platform.

Read the article on page 3 of this issue and learn how our multiplex kits for the Luminex® platform can advance your studies of cellular metabolism.

Get the complete package at www.millipore.com/magbeads



Multiplexed Quantification of Oxidative Phosphorylation Parameters as a Mechanistic Indicator for Drug-Induced Mitochondrial Toxicity

Wei Zheng, Jue Wang, Lothar Goretzki, Gabriela Korzus Merck Millipore Rod Capaldi, James Murray Mitosciences, Eugene, OR

Introduction

Mitochondrial toxicity is a problem that is receiving growing attention. Evidence shows that mitochondrial malfunction is linked to several chronic diseases, such as diabetes, cancer and neurodegenerative disorders. Recent studies show that many widely prescribed therapeutics have "off-target" effects on mitochondria that impair function through several mechanisms, including affecting oxidative phosphorylation (OXPHOS), a key mitochondrial function.

OXPHOS produces more than 95% of the conserved cellular energy in the form of ATP under normal conditions. This process involves five different protein complexes: NADH ubiquinone oxidoreductase (Complex I), succinate ubiquinone oxidoreductase (Complex II), ubiquinone cytochrome c oxidoreductase (Complex III), cytochrome c oxidase (Complex IV) and ATP synthase (Complex V). Nicotinamide nucleotide transhydrogenase (NNT) is a nuclear-encoded mitochondrial protein involved in detoxification of reactive oxygen species (ROS). OXPHOS is tightly controlled by transcriptional, post-translational and substrate feedback regulation. Due to the dual genetic origins of OXPHOS enzymes from both nuclear and mitochondrial DNA, the mitochondrial DNA and its OXPHOS protein products are specifically susceptible to toxicity induced by a variety of drugs including antiviral and antibiotic compounds. Not surprisingly, there is a growing need for assay tools that enable convenient measurement of key mitochondrial proteins in the drug development process in order to reduce late-stage drug attrition and safety liability due to mitochondrial toxicity. However, suitable high-throughput approaches have not been available.

Based on Luminex® xMAP® technology, we developed the Human Oxidative Phosphorylation 6-plex Panel. We used the panel to profile the mitochondrial safety of various classes of drugs in HepG2 cells: chloramphenicol (antibiotic), dideoxycytidine (ddC, an antiretroviral drug), and two glitazones (anti-diabetes class of drugs). Our results show that this multiplex assay is an accurate, reproducible method for quickly obtaining insight into potential mitochondrial toxicity of drug candidates.

Methods

Assay development:

A multiplex immunoassay OXPHOS 6-plex panel was developed against oxidative phosphorylation complexes: Complex I, II, III, IV, V and NNT with Luminex* xMAP* technology.

Sample treatment and analysis:

HepG2 hepatocellular carcinoma cells were cultured to 95% confluency then treated with either 20 μ M of chloramphenicol (Merck Millipore, Cat. No. 220551) for 6 days, or 20 μ M of ddC (2'–3'-dideoxycytidine, Sigma-Aldrich, Cat. No. 308358) for 6 days, during which the cells were split in conditioned media if necessary. In addition, HepG2 cells were cultured and treated with two members of the thiazolidinedione class of anti-diabetes drugs, rosiglitazone (Cayman Chemical, Cat. No. 71740, 50 μ M for 2 days) and troglitazone (Merck Millipore, Cat. No. 648469, 20 μ M for 2 days). DMSO mock-treated cells were used as control.

At the end of the treatment, the cell lysates were harvested. Equal amounts of cell lysate were analyzed in triplicate either with the Human OXPHOS Panel (6-plex) or with ELISAs following the recommended assay protocols to determine the quantity of each analyte. All assays were read using the Luminex 200TM instrument with data acquisition software. Drug-induced mitochondrial toxicity was evaluated by normalizing the quantity of each analyte to mock-treated cells and reporting the results as percentages of the mock-treated values.

Results

HepG2 hepatocellular carcinoma cells were treated with chloramphenicol, ddC, rosiglitazone and troglitazone, and analyzed with the OXPHOS panel and ELISAs. The data from the OXPHOS panel were consistent with ELISA data as well as those from the activity assay and the cellular oxygen consumption study (data not shown).

Chloramphenicol and ddC have known cytotoxic effects. Our results, as expected, indicated that chloramphenicol clearly induced mitochondrial toxicity (as demonstrated by significant reduction of Complex I and IV) while Complex II, III, V and NNT remained relatively stable (Figure 1). Figure 2 shows that ddC clearly induced mitochondrial toxicity (as demonstrated by significant reduction of Complex I, III and IV) while Complex II, V and NNT remained relatively stable.

HepG2 cells were cultured and treated with two members of the thiazolidinedione class of anti-diabetes drugs, rosiglitazone and troglitazone. Drug-induced mitochondrial toxicity was evaluated as described in the methods section. Both drugs caused reductions in the expression levels of OXPHOS components; however, the specific components affected varied. Rosiglitazone caused the most dramatic reductions in Complex IV, V, and NNT (Figure 3A), while troglitazone affected almost all tested components except for Complex III (Figure 3B).

Antibiotic-Induced Mitochondrial Toxicity

A Chloramphenicol 6 day 20 μM 200 OXPHOS Panel 150 T 7 50

Complex III

Complex IV

Complex V

¥

B Chloramphenicol 6 day 20 μM

Complex I

Complex II

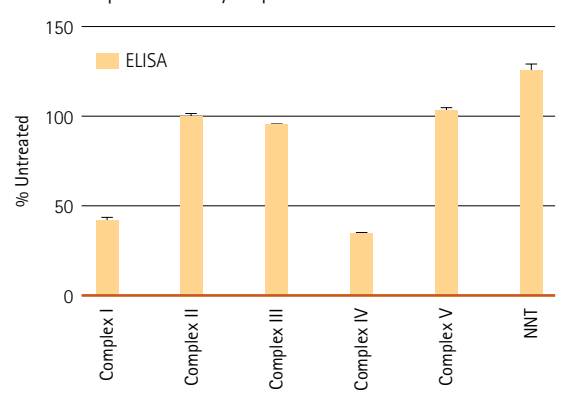
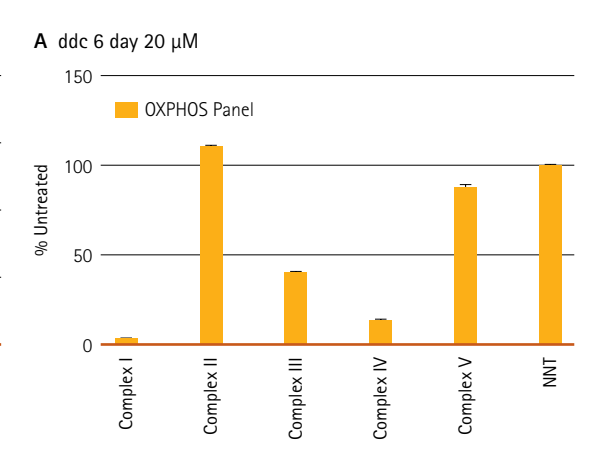
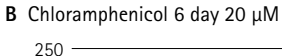


Figure 1. Significant reduction of Complex I and IV in chloramphenicol-induced mitochondrial toxicity. 1A shows results obtained using the Oxidative Phosphorylation panel, while 1B shows results obtained using ELISA assays. Data are representative of 5 replicates and error bars indicate standard deviation (SD).

Antiviral Drug-Induced Mitochondrial Toxicity





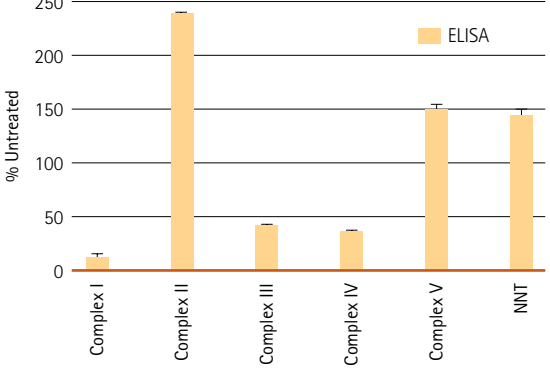
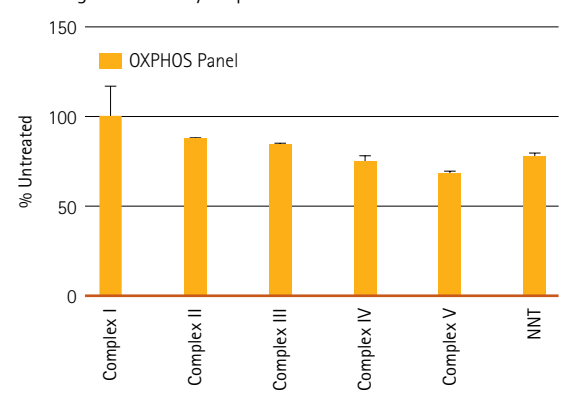


Figure 2. Significant reduction of Complex I, III and IV in antiviral drug-induced mitochondrial toxicity. 1A shows results obtained using the Oxidative Phosphorylation panel, while 1B shows results obtained using ELISA assays. Data are representative of 5 replicates and error bars indicate standard deviation (SD).

Troglitazone was withdrawn from the European market in 1997, and from the U.S. market in 2000, because of hepatotoxicity. Rosiglitazone has shown some hepatotoxic effects and more significantly, cardiovascular side effects^{1,2}. As a result, the European Medicines Agency (EMEA) recommended the withdrawal of rosiglitazone from the market in 2010. Although the U.S. Food and Drug Administration (FDA) has refrained from making a similar decision, it has required relabeling of rosiglitazone with additional warnings.

Glitazone-Induced Mitochondrial Toxicity

\boldsymbol{A} Rosiglitazone 2 day 50 μM



B Troglitazone 2 day 20 μM

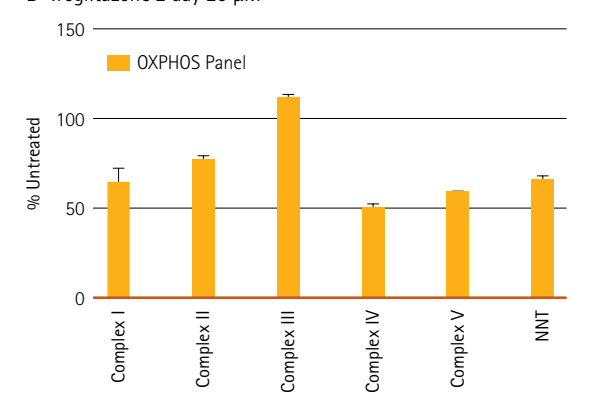


Figure 3. Comparison of mitochondrial toxicity induced by rosiglitazone and troglitazone shows that troglitazone is significantly more toxic than rosiglitazone. Data are representative of 5 replicates and error bars indicate standard deviation (SD).

Summary

We have developed the Human Oxidative Phosphorylation 6-plex Panel to quantify OXPHOS Complex I, II, III, IV, V and NNT simultaneously with accuracy and precision using Luminex® xMAP® technology. The Human OXPHOS Panel enables simultaneous multiplex detection of respiratory chain complexes, a mechanistic indicator for mitochondrial toxicity. The OXPHOS quantification profile determined by the Human OXPHOS Panel correlates well with pre-established complex activity and cellular oxygen consumption data.

The Human OXPHOS Panel detects mitochondrial toxicity induced by antibiotic, antiretroviral, and the glitazone class of anti-diabetes drugs. Furthermore, it provides mechanistic insights into drug-induced mitochondrial toxicity. The data suggest that the Human OXPHOS 6-plex Panel is suitable as a novel drug safety screening tool to identify potential off-target effects on mitochondrial respiratory chain complexes for new antiviral, antibiotic and other drug molecule leads.

References

- Baselt R. Disposition of Toxic Drugs and Chemicals in Man, 8th edition, Biomedical Publications, Foster City, CA, 2008, pp. 1399–1400.
- Graham DJ et al. Risk of acute myocardial infarction, stroke, heart failure, and death in elderly Medicare patients treated with rosiglitazone or pioglitazone. Journal of the American Medical Association (JAMA). 2010 Jul 28; 304(4):411-8.

FEATURED PRODUCTS

Available from www.millipore.com

Description	Catalogue No.
Luminex 200™ Instrument with xPONENT® Data Acquisition Software	Visit www.millipore.com/milliplex or call 1-800-MILLIPORE to request a quote
MILLIPLEX® MAP Oxidative Phosphorylation Magnetic Bead Panel	Coming soon

Available from www.merck4biosciences.com

Description	Catalogue No.
Chloramphenicol	220551
Troglitazone	648469

Functional Human Oligodendrocyte Progenitors Provide Optimized *In Vitro*Differentiation For Studies of Myelinization

Christine Chen Merck Millipore

Introduction

Neural stem cells (NSCs) have been intensely studied for their therapeutic potential in neurodegenerative disease and brain injury. Depending on the combination of microenvironment and growth stimuli, these cells can undergo neurogenesis and replace damaged cells. In the central nervous system, neurogenesis alone is not sufficient to repair neuron damage¹. Functional neurons need to be protected by a myelin sheath, which is synthesized by oligodendrocytes, in order to successfully deliver a long-distance action potential. Therefore, understanding oligodendrocyte development is a necessary milestone towards developing clinical and pharmaceutical treatments for neurodegenerative pathologies.

Most myelination studies use primary oligodendrocytes isolated from rodent systems because they are easily obtained. However oligodendrocytes derived from rodents may not respond to growth factors in the same way as to human oligodendrocytes, and the developmental timelines are expected to be different in the two systems². For example, while human oligodendrocytes take several weeks to mature in cultured brain slice, rodent oligodendrocyte progenitors mature within one week *in vitro*³. It is thus important to validate and study diseases affecting myelination using a human model cell system.

Previously, we have shown that highly enriched oligodendrocyte progenitor cells (OPCs) can be derived from human embryonic stem cells (hESCs)⁴. These cells are positive for multiple oligodendroglial markers, such as NG2, O4, Sox10 and GalC. Over 70% cells express progenitor to pre-oligodendrocyte markers. Withdrawal of growth factor from culture conditions initiates spontaneous differentiation. After two weeks of spontaneous

differentiation, about 30% of the cells start to express markers for mature oligodendrocytes, such as MBP and PLP/DM20, as detected by RT-PCR and by immunofluorescent staining.

In this report, we extended our characterization of this system for oligodendrocyte development from the gene expression level to functional analysis. Myelin basic protein (MBP) was used as a marker for OPC maturation and as an index for myelination. Using a coculture system, we showed that human OPC developed into mature oligodendrocytes that produced MBP around the axon in primary rat neuron cultures. In addition, we also set up an assay to illustrate how these cells could be used to screen for molecules that exert effects on oligodendrocyte differentiation and maturation. Overall, we provided more evidence to demonstrate the functionality of our human OPC model and how it could be applied to facilitate *in vitro* studies of oligodendrocyte biology.

Materials and Methods

Cell Line and Culture Conditions

Human ES cell-derived OPCs (Merck Millipore Cat. No. SCR600) were cultured in Human OPC Expansion Medium (Merck Millipore, Cat. No. SCM107) with an initial seeding density of 1–2 x 10⁴ cells/cm². Upon confluence, cells were harvested with Accutase™ (Merck Millipore, Cat. No. SCR005) and cultured for 1 to 2 passages before differentiation.

In Vitro Myelination Assay

12 mm cover glasses were acid-treated with 1N HCl overnight, rinsed with Milli- 0° H $_2$ 0 and then sterilized with autoclaving. Cover glasses were air dried before being coated with 0.1% poly-L lysine (Sigma) at room temperature for 1 hour and then washed with sterile

distilled water. 1 x 10⁵ primary E19 rat hippocampal neurons were plated on the poly-L-lysine coated cover glass in each well of a 4-well plate (Thermo Fisher Scientific) in Dulbecco's Modified Eagle Medium (DMEM) with 10% heat-inactivated horse serum. 24 to 48 hours after plating, cells were transfected with 1 µg of pCAG-GFP plasmid using Lipofectamine™ 2000 (Life Technologies) following the manufacturer's protocol. 24 hours posttransfection, approximately 10-20% of the primary neurons were GFP-positive. Four days after transfection, 2 x 10⁴ human OPCs were seeded to the plate and the neuronal culture medium was replaced with the Human OPC Spontaneous Differentiation Medium (Merck Millipore, Cat. No. SCM106). Human OPCs and rat primary neuron coculture was left at 37 °C in a 5% CO₂ tissue culture incubator for 21 days with medium changes every 2 to 3 days. Cells were fixed in the same medium containing 2% paraformaldehyde at 37 °C for 15 minutes followed by four washes of 1X phosphate-buffered saline (PBS).

Screening Small Molecules for Effects on Oligodendrocyte Differentiation

24-well plates (Thermo Fisher) were coated with 10 μg/mL poly-L-ornithine (Sigma) for 2 hours at room temperature before being replaced with a 10 μg/mL mouse laminin (Merck Millipore, Cat. No. CC095) solution incubated at room temperature overnight. Wells were washed with 1X PBS prior to receiving the cells. 2 x 10⁴ human OPCs were seeded in each well of the coated 24-well plate in Human OPC Expansion Medium (Merck Millipore, Cat. No. SCM107). Twenty-four hours after plating, the expansion medium was replaced with the Human OPC Spontaneous Differentiation Medium (Merck Millipore, Cat. No. SCM106) containing the following small molecules or growth factors. MEK1/II inhibitor, PD0326901 (Merck Millipore, Cat. No. 444966), 2, 3-bis (4-hydroxyphenyl)-propionitrile; (DPN, Sigma) and 1, 3, 5-Tris (4-hydroxyphenyl)-4-propyl-1H-pyrazole (PPT, Sigma). The stock solutions were prepared with dimethyl sulfoxide at 10 mM and diluted in medium prior adding to cells. The medium was changed every two to three days for two weeks before fixation.

Immunofluorescent Staining and Image Acquisition

In vitro myelination assay:

Antibodies are listed in Table 1. Samples from the *in vitro* myelination assay were blocked and permeabilized with 1X PBS containing 5% normal goat serum, 5% bovine serum albumin (BSA) and 0.2% Triton X-100 for two hours at room temperature. Samples were first incubated with anti-MBP antibody (Merck Millipore, Cat. No 05-675) at 4 °C overnight, washed 3 times with 1X PBS and incubated with goat anti-mouse Cy5-conjugated secondary for one hour

at room temperature. Human nuclei were stained using a fluorescent conjugated human nuclei-specific antibody (Merck Millipore, Cat. No. MAB1281) with DyLight® Fluor Antibody Labeling Kits for 2 hour at room temperature. Excess antibody was removed with three washes of 1X PBS. Nuclei were stained with Hoechst 33342 dye at 1:2000 dilutions. 3D images were acquired by a confocal microscope (Leica DMI 4000; 40x objective, 275 x 140 µm; 63x objective, 174.6 x 174.6 µm) and reconstructed by the Leica AF. To analyze the degree of myelination, MBP staining intensities were measured by line scanning cultures containing rat neurons only and rat neuron and human OPC co-culture by Leica AF.

Two-week differentiation assay:

Samples were blocked in 5% normal goat serum and 5% BSA in 1X PBS; Triton X-100 (0.2%) was included for intracellular staining. After 2 hours blocking, cells were incubated with primary antibody overnight at 4°C. Secondary staining was performed with 2.5 µg/mL goat anti-mouse (Alexa Fluor® 555-conjugated, red) and goat anti-rabbit (Alexa Fluor® 488-conjugated, green) for 1 hour at room temperature. Directly conjugated antibody was applied for one hour at room temperature. Nuclei were counterstained with Hoechst 33342 dye at 1:2000 dilution. Images were acquired with an epifluorescent microscope equipped with CCD camera (Leica DMI 6000 AF with Hamamatsu Photonics ORCA) and 20x objectives.

Flow cytometry analysis:

106 cells were fixed in 2% paraformaldehyde at room temperature for 15 minutes, followed by three washes with 1X PBS. Cells were blocked with 2% FBS in 1X PBS for 5 minutes at room temperature with or without 0.2%

Antibody	Species	Subcellular Location	Dilution	Merck Millipore Catalogue No.
04	Mouse IgM	Surface	1:20	MAB345
NG2	Rabbit IgG	Surface	1:200	AB5320
GalC	Mouse IgG	Surface	1:200	MAB342
Sox10	Rabbit IgG	Nuclei, cytoplasmic	1:200	AB5727
MBP	Mouse IgG, ascite	Surface	1:20	05-675
Olig2	Rabbit IgG	Perinuclei	1:100	AB9610
PLP/DM20	Mouse IgG	Surface	1:100	MAB388
PLP	Chicken	Surface	1:100	AB15454
Human nuclei	Mouse IgG	Nuclei	1:100*	MAB1281
MOG	Mouse IgG	Surface	1:50	MAB5680
MAP2	Mouse IgG	Intracellular cytoskeleton	1:200	MAB3418
GFAP	Mouse IgG	Intracellular cytoskeleton	1:200*	MAB3402RX

*direct conjugate

Table 1. Antibodies used in this study

Triton X-100. Cells were transferred to ice and 1:100 antibody was added to each reaction for 1 hour. Cells were washed twice with blocking solution, then 1:200 secondary antibody (goat anti-rabbit or goat anti-mouse Alexa Fluor® 488-conjugated) was added and incubated for 30 minutes. Cells were washed once with blocking solution before analysis with the guava easyCyte™ 8HT benchtop flow cytometer. Secondary antibody only was used as a control.

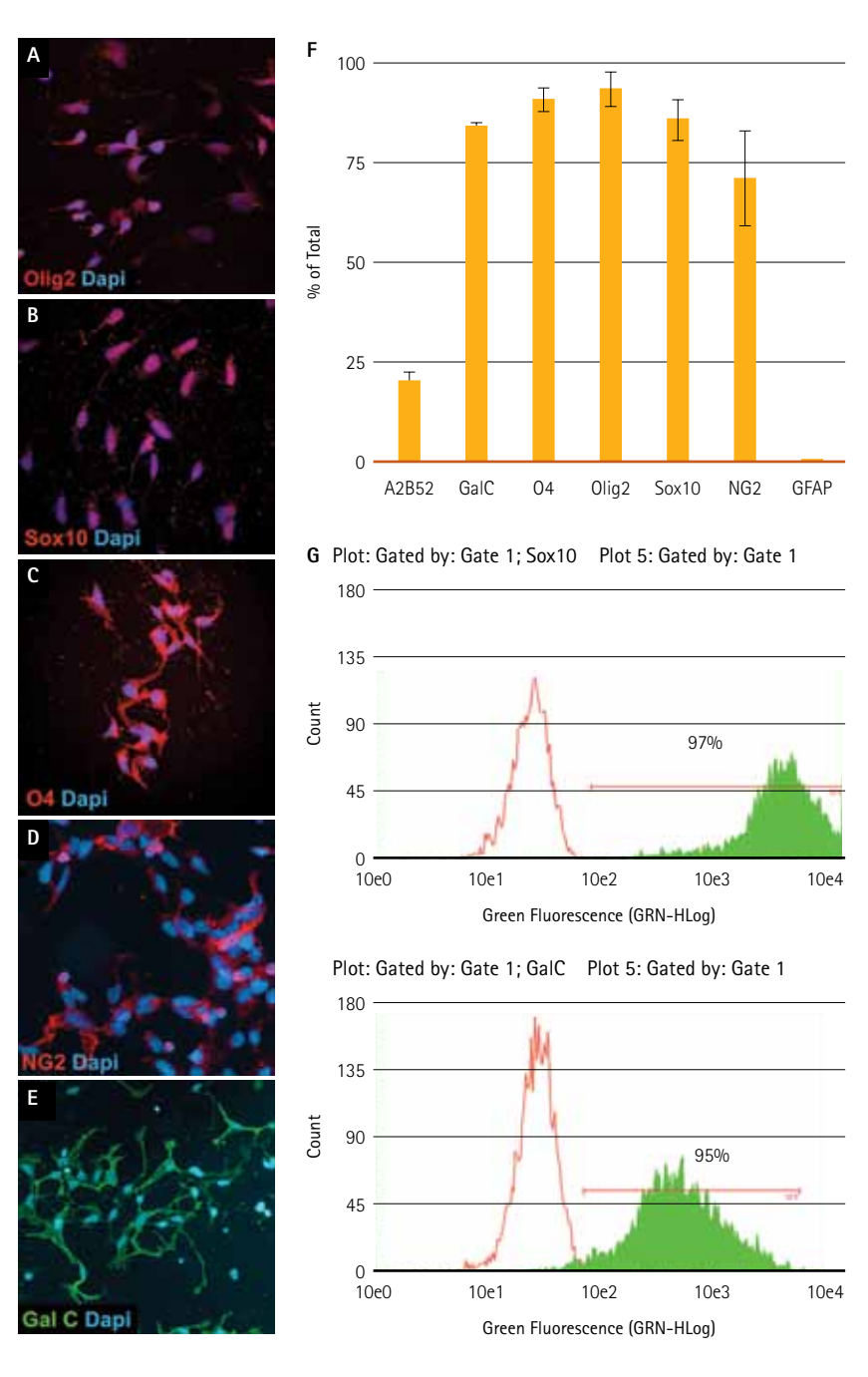


Figure 1. Characterization of human ES cell-derived oligodendrocyte progenitor cells.

Results and Discussion

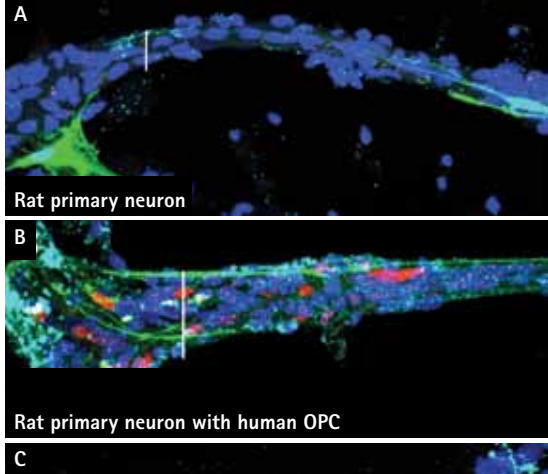
Characterization of human ES cell-derived OPCs

We established a protocol to derive oligodendrocyte progenitor cells (OPCs) from human embryonic stem cells with a consistent level of progenitor marker expression (Figure 1). These cells possessed a stable proliferation rate and appeared to be in the early-to-intermediate progenitor stages. Cells could be cultured in Human OPC Expansion Medium for 2 to 3 passages without changing their proliferation rate or differentiation capacity (data not shown).

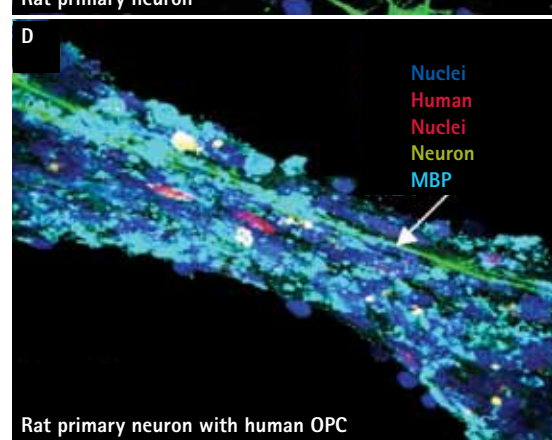
Oligodendrocyte progenitor cells were plated at 10⁴/cm² onto poly-L-ornithine- and laminin-coated 8-well chamber slides. Cells were fixed 24 to 48 hour post seeding. These cells expressed early oligodendrocyte progenitor markers (A) Olig2, (B) Sox10, (C) O4 and (D) NG2. Significant numbers of cells expressed the intermediate oligodendrocyte marker (E) GalC. Three randomly selected fields were quantified. Nuclei number by Hoechst staining were used to count the total number of cells. (G) Flow cytometry analysis of OPC with Sox10 marker. (H) Flow cytometry analysis of OPCs with GalC marker.

Myelination of neurons by human ES cell-derived oligodendrocytes

Rat primary neurons isolated from the embryonic hippocampus are mostly pyramidal neurons that have a distinctive morphology composed of single axons and multiple dendrites. To facilitate identification of the rat primary neurons, green fluorescent protein (GFP) was introduced by transient transfection. 10%-20% cells were successfully transfected and GFP expression was stable for the period of observation. Human ES cell-derived OPCs were added to the rat primary neuronal culture at a ratio of 1:5. Three weeks after initiating coculture, we analyzed the relative degree of myelination by immunofluorescent staining. Myelin basic protein (MBP) is a major component of the myelin sheath. In the absence of Human OPCs, rat primary neuronal cultures exhibited little to no staining for MBP (Figure 2 A, C, E). In contrast, in the coculture containing GFP-labeled axons and human OPCs, significant MBP staining was observed (Figure 2B, D, E). The expression of MBP colocalized with nuclei, providing evidence that MBP is expressed from human OPCs. We also observed MBP expression in differentiated human OPCs (data not shown). These data suggested that in the presence of mature or developing axons, human ES cell-derived OPCs can be further maturated to functional oligodendrocytes that are capable of producing myelin to protect the axons.



Rat primary neuron



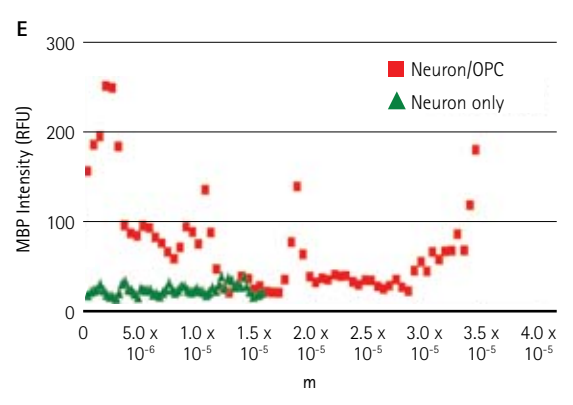


Figure 2. In vitro myelination assay.

Reconstructed 3D images of (Leica DMI 4000; 40x objective, 275 x 140 μ m; 63x objective, 174.6 x 174.6 μ m) rat primary neurons only (A, C) and rat primary neurons cocultured with human OPCs at 5:1 ratio for three weeks (B, D). All samples were stained with human specific nuclei antibody (red) and myelin basic protein specific antibody (cyan). MBP intensities (E) were measured by line scanning on cultures containing rat primary neurons only (A) and rat primary neurons with human OPCs (B). GFP labeled axons are indicated by the white arrow. The intensity of MBP greatly increased on the axons that are cocultured with human OPCs.

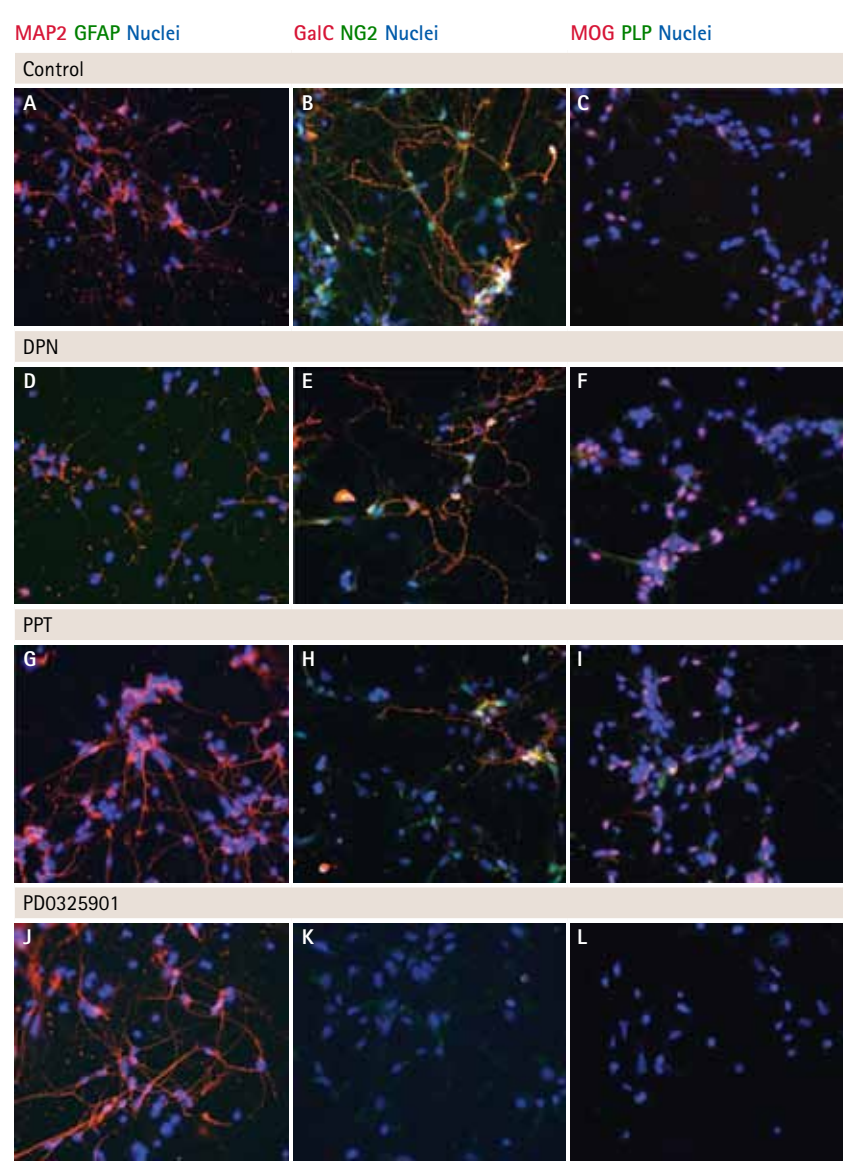


Figure 3. Small molecule screening for OPC *in vitro* maturation. Human OPCs were differentiated in Human OPC Spontaneous Differentiation Medium (control, A-C) for two weeks. Media contained either 100 nM DPN (D-F), 100 nM PPT (G-I) or 1 μ M PD0325901 (J-L).

$ER\beta$ activation may be involved in oligodendrocyte maturation

The estrogen receptor beta (ER β) signaling cascade has been implicated in oligodendrocyte survival and maturation in the mouse model⁵. Activation of ER β increases the expression of TrKB and IGF-1 receptors, which then signal via MEK/ERK kinase and AKT/mTOR cascades to mediate cell proliferation and survival *in vivo*⁶. Here, we tested the effect of ER β activation in human OPC differentiation. ER β agonist (2, 3-bis (4-hydroxyphenyl)-propionitrile; DPN) or ER α agonist (1, 3, 5-Tris (4-hydroxyphenyl)-4-propyl-1H-pyrazole; PPT) was included in the differentiation medium at 100 nM. After two weeks of differentiation, cells were fixed and stained with neuronal (MAP2), astroglial (GFAP), early/intermediate oligodendrocyte (GalC/NG2) and late oligodendrocyte (MOG/PLP) markers.

Activation of ER β by DPN resulted in a higher number of MOG-positive cells and concomitant decrease in MAP2-positive cells (Figure 3D and 3F). Activation of ER α resulted in an increase in MOG-positive cells and MAP2-positive cells (Figure 3G and 3I). In contrast, use of the inhibitor PD0325901, which blocks the MEK/ERK kinase, abolished MOG and GalC/NG2 expression but exerted a limited effect on the percentage of MAP2 positive cells (Figure 3J-L). Our preliminary results are consistent with previously published studies linking activation of ER β to oligodendrocyte maturation and the downstream effects of MEK/ERK kinase activity in the signaling process.

Conclusion

In summary, we showed that Merck Millipore's human oligodendrocyte progenitor cells are capable of myelination, supporting the functional utility of these cells as a relevant model system for studying neural development and neuroregeneration. The cells may also be used to screen for molecules that promote or inhibit human OPC survival and differentiation. Our current efforts are in identifying those molecules that would increase OPC differentiation.

References

- Galvan V, Bredesen DE. Neurogenesis in the adult brain: implications for Alzheimer's disease. CNS Neurol Disord Drug Targets. 2007 Oct;6(5):303–10.
- Chandran, S. et al. Differential generation of oligodendrocytes from human and rodent embryonic spinal cord neural precursors. Glia. 2004; 47:314–324.
- Jakovcevski, I. et al. Oligodendrocyte development and the onset of myelination in the human fetal brain. Front Neuroanat. 2009; 3:5.
- Chen, C. et al. Derivation of oligodendrocyte progenitor cells from a human neural stem cell line. Cellutions. 2010; 4:3-6.
- 5. Tiwari-Woodruff, S., et al. Differential neuroprotective and antiinflammatory effects of estrogen receptor (ER) α and ER β ligand treatment. Proc Natl Acad Sci USA. 2007; 104:14813–14818.
- Crawford, D. K. et al. Oestrogen receptor beta ligand: a novel treatment to enhance endogenous functional remyelination. Brain. 2010; 133:2999–3016.

FEATURED PRODUCTS

Available from www.millipore.com

Description	Catalogue No.
Human Oligodendrocyte Differentiation Kit	SCR600
Human OPC Expansion Medium	SCM107
Accutase™	SCR005
Human OPC Spontaneous Differentiation Medium	SCR106

Fast and Gentle Enrichment Assays for Isolating and Staining Native Protein-Cytoskeleton Associations

Haizhen Liu, Karyn Huryn, Jun Ma and Luke Armstrong Merck Millipore

Abstract

The core mammalian cytoskeleton consists of actin microfilaments, focal adhesions, microtubules, and intermediate filaments, which are constructed through the assembly of free subunits of actin, tubulin and keratin-related proteins into highly organized arrays. The biochemical changes of these proteins during assembly are incompletely understood, as the presence of both free and assembled subunits within the cell complicates analysis. We developed two reagent kits for selectively separating soluble cytosolic proteins from adherent cells, enabling more sensitive biochemical analysis (including Western blot and mass spectrometry) and imaging analysis of the insoluble cytoskeleton and associated proteins in their native conformations. We demonstrate that these kits can greatly increase the ability to detect and study low abundance actin-associated proteins, which are typically masked in conventional Western blot analysis of whole cell lysates, and can greatly reduce the background typically seen in immunofluorescence staining of whole cells.

Introduction

The actin cytoskeleton is a highly dynamic network composed of actin polymers and a large variety of associated proteins. The actin cytoskeleton mediates a variety of essential biological functions in all eukaryotic cells, including intra- and extra-cellular movement and structural support^{1,2}. To perform these functions, the organization of the actin cytoskeleton must be tightly regulated, both temporally and spatially. Many proteins associated with the actin cytoskeleton are thus likely targets of signaling pathways that control actin assembly. Actin cytoskeleton assembly is regulated at multiple levels, including the organization of actin monomers (G-actin) into actin polymers and the super-organization of actin polymers into a filamentous network (F-actin - the major constituent of microfilaments)³. This super-organization is mediated by actin side-binding or cross-linking proteins^{4,5,6}. The actin cytoskeleton rapidly changes shape and organization in response to stimuli and cell cycle progression. Therefore, a disruption of its normal regulation may lead to cell transformation and cancer. Transformed cells have been shown to contain less F-actin than untransformed cells and exhibit atypical coordination of F-actin levels throughout the cell cycle⁷. Orientational distribution of actin filaments within a cell is, therefore, an important determinant of cellular shape and motility.

Focal adhesions and adherens junctions are membrane-associated complexes that serve as nucleation sites for actin filaments and as cross-linkers between the cell exterior, plasma membrane and actin cytoskeleton⁸. The function of focal adhesions is structural, linking the extracellular matrix (ECM) to the actin cytoskeleton on the inside of the cell. Focal adhesions are also sites of signal transduction, initiating signaling pathways in response to adhesion. Focal adhesions consist of integrin-type receptors that are attached to the extracellular matrix and are intracellularly associated with protein complexes containing vinculin (universal focal adhesion marker), talin, α -actinin, paxillin, tensin, zyxin and focal adhesion kinase (Figure 1)^{9,10}.

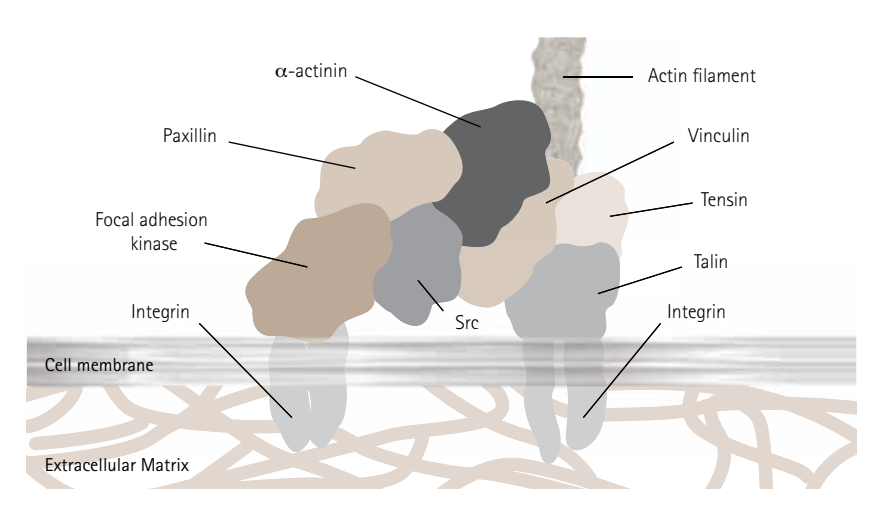


Figure 1. Composition of Focal Adhesion.

Studying the proteins that associate with and regulate the actin cytoskeleton has traditionally been difficult because the cytoskeleton is insoluble in detergents like Triton-X100. Many actin regulatory proteins/phosphoproteins, upon activation, move from the soluble cytoplasmic compartment to the insoluble actin cytoskeleton. The insolubility of these important proteins has made it difficult to study their biochemical changes, such as phosphorylation and nitrosylation, upon binding to the actin cytoskeleton. Here we describe a cytoskeleton purification and enrichment method that enables the selective enrichment of cytoskeleton-associated proteins for detailed protein biochemical analyses. This method provides the means to directly study this important pool of proteins in normal and diseased cytoskeletons, without major disruption to the native cytoskeleton conformation or the native cytoskeleton-protein associations.

Materials and Methods Reagents

The ProteoExtract® Cytoskeleton Enrichment and Isolation Kit provides the necessary extraction buffers to quickly, gently and selectively remove soluble cytoplasmic and nuclear proteins from the cell, while retaining focal adhesion and actin-associated proteins. Vimentin and GAPDH antibodies are also provided as markers for the cytoskeleton and cytosol, respectively, for Western blot analysis. The enriched cytoskeleton proteins can also be subjected directly to mass spectrometry analysis, or further enzyme digested prior to analysis. The ProteoExtract® Native Cytoskeleton Enrichment and Staining Kit also provides the necessary reagents to gently enrich and retain the cytoskeleton and associated proteins in their native conformations. Additionally, the staining kit provides labeled phalloidin and labeled antibodies against vinculin and GAPDH as markers for visualization and colocalization of the actin cytoskeleton, focal adhesions and cytosol, respectively, for immunofluorescence analysis.

Cell culture and cytoskeleton enrichment

Human HeLa cells were grown in Dulbecco's Modified Eagle Medium (DMEM) complete medium in 100 mm culture dish until 80–90% confluence. The cells were gently washed twice with 2 mL of cold 1X Dulbecco's Phophate Buffered Saline (DPBS). Cold 1X Cellular Extraction Buffer (0.25 mL per plate) was added to the cells and incubated for 1.5 minutes on ice. Buffer was collected and labeled as Soluble Compartment (S). 0.5 mL 1X Cytoskeleton Wash Buffer was added to the cells and then pooled with the Soluble Compartment. Nuclear Extraction Buffer

(0.25 mL per plate) was added to the cells, and incubated on ice for 10 minutes. This fraction was collected and labeled as Nuclear Compartment (N). Cells were washed twice with 2 mL of 1X Cytoskeleton Wash Buffer.

Enriched cytoskeleton isolation

To isolate the enriched Cytoskeleton compartment, 0.25 mL of Cytoskeleton Solubilization Buffer was added to the cells following the Cytoskeleton Wash Buffer step, and pipetted up and down for maximum solubilization. This fraction was collected and labeled as Cytoskeleton Compartment (C). Protein concentrations of all collected compartments were determined by A_{280} and stored at -80 °C until further application as described below.

Enriched native cytoskeleton fixation

To visualize the enriched native cytoskeleton, human HeLa cells were grown in DMEM complete medium in 8-well glass chamber slides until 80–90% confluence. Extraction of soluble and nuclear compartments was performed as above, except that these fractions were discarded by aspirating at each step. The adherent insoluble cytoskeleton remaining attached to the chamber slide was fixed by addition of 0.25 mL 4% paraformaldehyde to each well following the last Cytoskeleton Wash Buffer step to fix the cells. After a 30-minute incubation at room temperature, the cells were washed with 0.25 mL of 1X DPBS per well.

Immunostaining and visualization

After fixing the native cytoskeleton, the cells were washed twice with 0.5 mL 1X Blocking/Permeabilization Buffer, and incubated with 0.25 mL/well diluted primary antibody in 1X Blocking/Permeabilization Buffer for 1 hour at room temperature. Washes and incubation with a dye-conjugated secondary antibody, TRITC-conjugated phalloidin (1:100) and DAPI (1:200), each provided in the staining kit, were performed to stain the actin cytoskeleton and remaining cell nucleus. Cover slips were mounted on slides with mounting fluid and visualized with a fluorescence microscope.

Western blot analysis

Following the enrichment of the cytoskeleton, collected cell compartments (S, N and C) were subjected to SDS-PAGE gel and transferred to a PVDF membrane. GAPDH and vimentin antibodies (provided in the kit) were used to detect cytosolic and intermediate filament proteins, respectively, using standard Western blotting procedures.

Results

We utilized these fast and convenient methods to enrich and either isolate or stain the native cytoskeleton-associated proteins, minimizing interference by soluble cytoplasmic and nuclear proteins (Figure 2). For biochemical analysis, fractions were collected in a stepwise process, whereas for imaging, the native cytoskeleton was chemically fixed on the culture surface. The entire extraction process could be completed in approximately 20 minutes.

Western blot analysis indicated that GAPDH was present in the cytoplasmic and nuclear fractions¹¹, whereas the intermediate filament protein vimentin was present exclusively in the cytoskeletal compartment (Figure 3). The ability to detect and study the low abundance cytoskeleton-associated proteins was greatly increased with this cytoskeleton enrichment and isolation method.

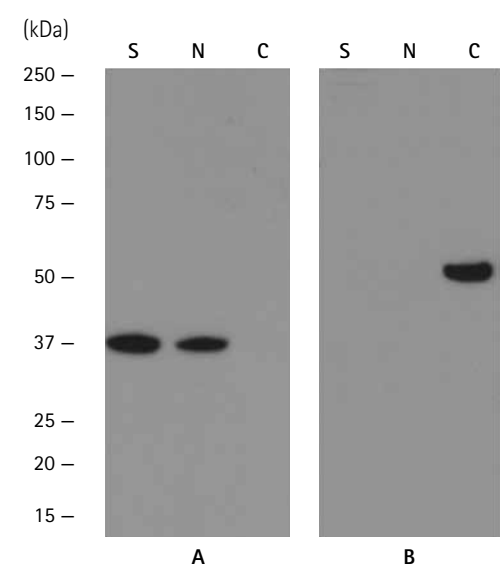


Figure 3. Western blot of compartmental proteins extracted from HeLa cells using ProteoExtract® Cytoskeleton Enrichment and Isolation Kit (Catalog No. 17–10195). Results indicate that GAPDH (Panel A) is present in the soluble cytoplasmic (lane S) and nuclear (lane N) fractions [11], and the intermediate filament protein Vimentin (Panel B) is present exclusively in the cytoskeletal compartment (lane C).

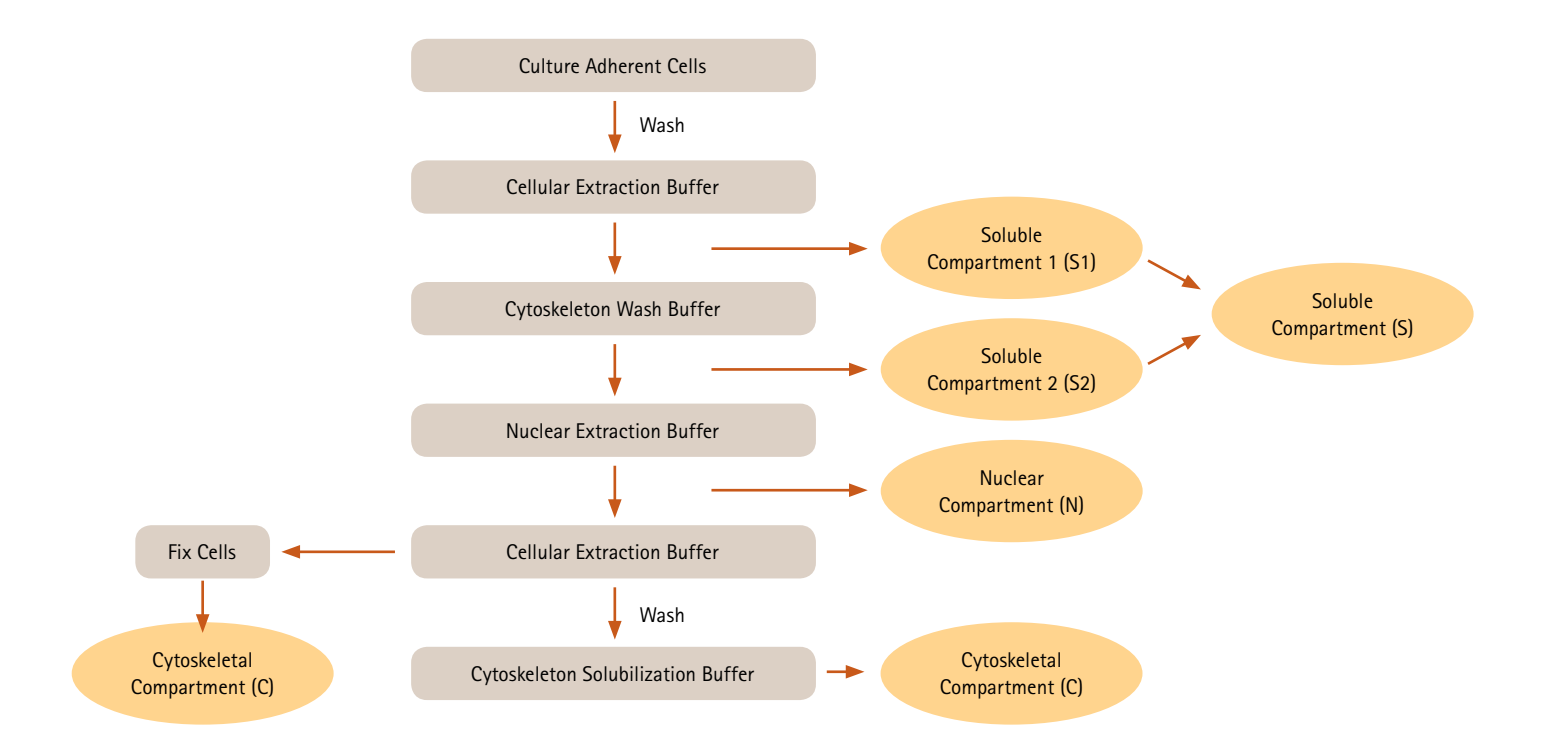


Figure 2. Cytoskeleton Enrichment Kit Procedure

The cytoskeleton enrichment and staining method greatly enhanced sensitivity of detection of focal adhesion and cytoskeletal proteins by removing soluble cytoplasmic and nuclear proteins. GAPDH is a cytosolic marker which was completely removed by the enrichment procedure (Figure 4, panel B, treated cells). Vimentin, an intermediate filament protein, was largely retained after the enrichment (Figure 5, panel B, treated cells).

Vinculin, an integral component of focal adhesion plagues, is involved in linkage of intergrin adhesion molecules to the actin cytoskeleton. Conventional whole-cell staining (Figure 6, panel B, non-treated cells) resulted in some focal adhesions detected on a diffuse background. With the ProteoExtract® Cytoskeleton Enrichment kit, the background staining due to soluble cytosolic pool of vinculin was significantly reduced, resulting in sensitive detection of insoluble vinculin solely at focal adhesions (Figure 6, panel B, treated cells). In addition, distribution of β -catenin, which anchors the actin cytoskeleton to cell-cell junctions, was restricted to cell-cell junctions (Figure 7, panel B, treated cells), as compared to the combination of diffuse and membrane-associated staining in non-treated whole cells (Figure 7, panel B, non-treated cells). Thus, this method for extraction of soluble proteins and enrichment of the insoluble cytoskeleton provided the means for more sensitive, accurate analysis of the important pool of proteins in cytoskeleton structure.

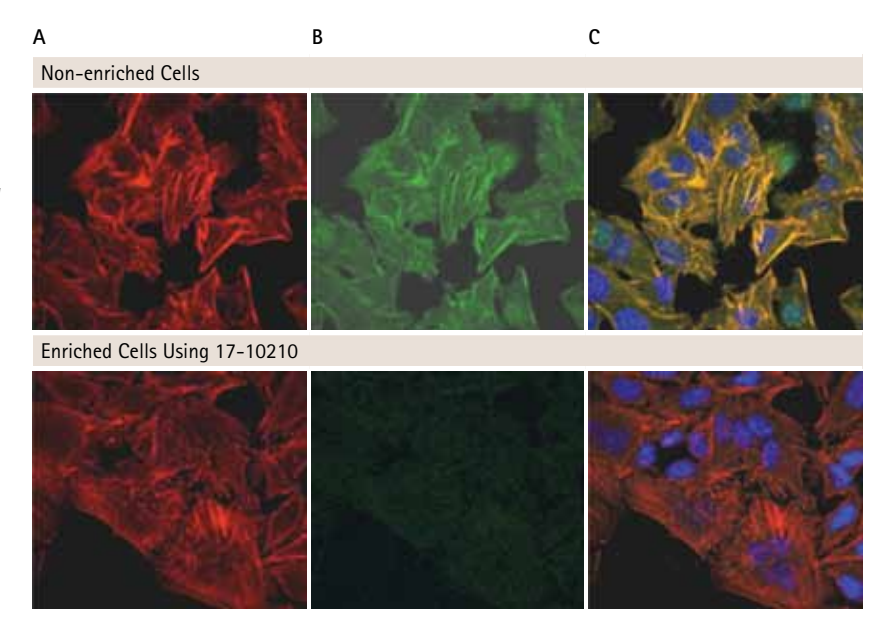


Figure 4. Confocal fluorescence microscopy of non-treated/enriched and treated/enriched HeLa cells. (A) F-actin was detected using TRITC-conjugated Phalloidin, (B) cytosolic protein was detected using GAPDH antibody as a cytosolic control and a FITC-conjugated secondary, (C) nuclear counterstaining was revealed with DAPI and all images were overlaid. Soluble cytosolic protein fraction (GAPDH) was successfully removed after enrichment using the ProteoExtract® Cytoskeleton Enrichment and Staining Kit.

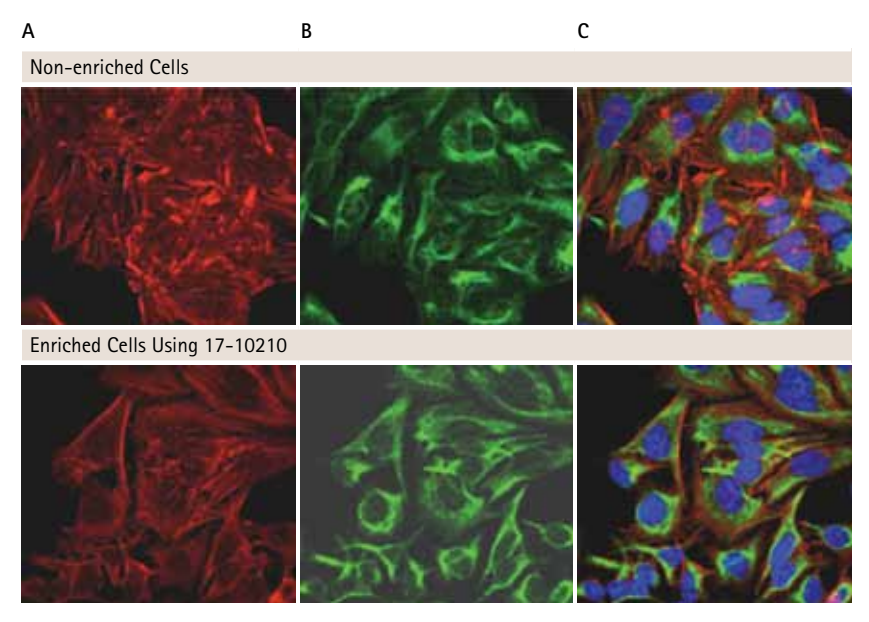


Figure 5. Confocal fluorescence microscopy of non-treated/enriched and treated/enriched HeLa cells. (A) F-actin was detected using TRITC-conjugated Phalloidin, (B) cytoskeletal protein was detected using Vimentin antibody and a FITC-conjugated secondary, (C) nuclear counterstaining was revealed with DAPI and all images were overlaid. Insoluble cytoskeletal protein fraction (vimentin) was successfully retained after enrichment using the ProteoExtract® Cytoskeleton Enrichment and Staining Kit.

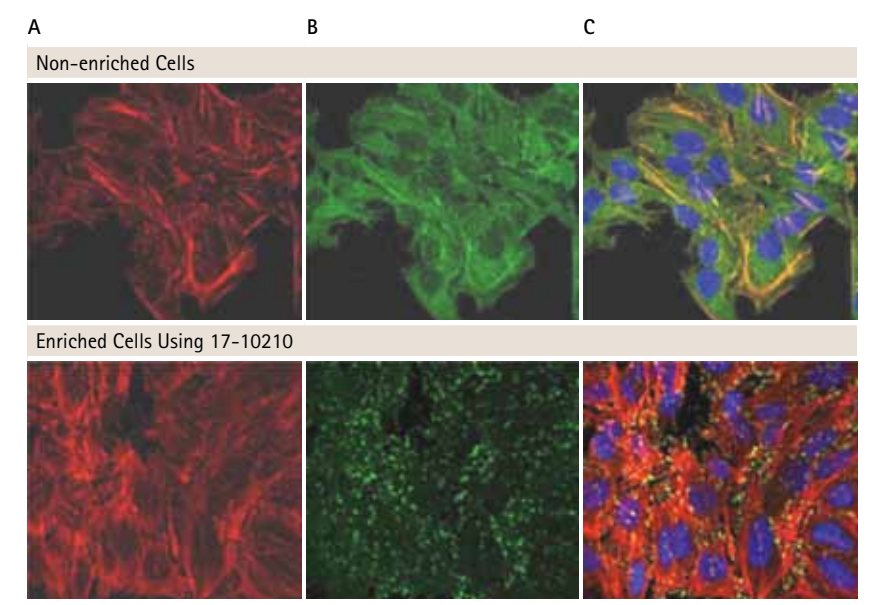


Figure 6. Confocal fluorescence microscopy of non-treated/enriched and treated/enriched HeLa cells. (A) F-actin was detected using TRITC-conjugated Phalloidin, (B) focal adhesion contacts were detected using Vinculin antibody and a FITC-conjugated secondary, (C) nuclear counterstaining was revealed with DAPI and all images were overlaid. Background due to soluble cytosolic fraction was significantly reduced after enrichment using the ProteoExtract® Cytoskeleton Enrichment and Staining Kit (Cat. No. 17-10210), resulting in clear detection of insoluble, actin-associated proteins (vinculin).

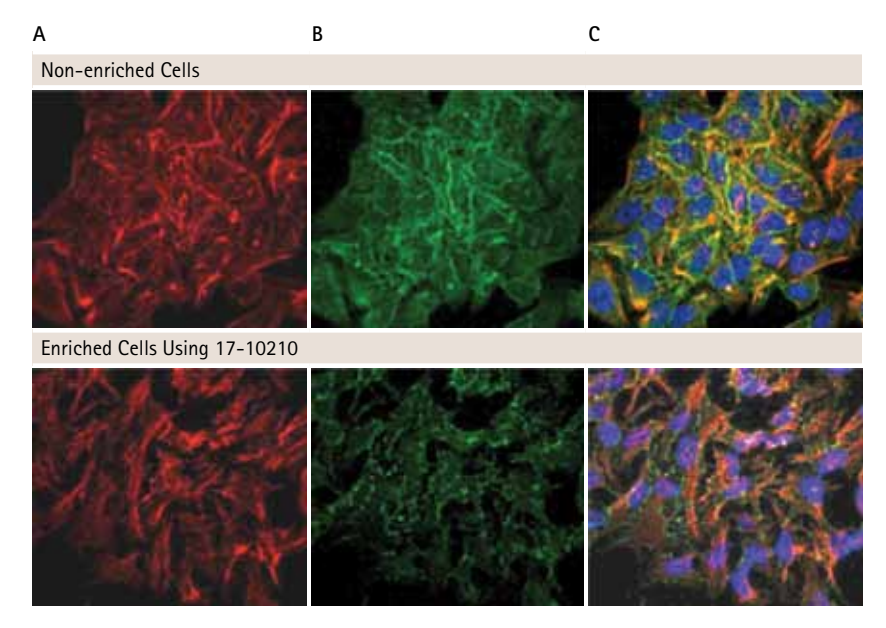


Figure 7. Confocal fluorescence microscopy of non-treated/enriched and treated/enriched HeLa cells. (A) F-actin was detected using TRITC-conjugated phalloidin, (B) cell junctions were detected using β -Catenin antibody and a FITC-conjugated secondary, (C) nuclear counterstaining was revealed with DAPI and all images were overlaid. Background due to soluble cytosolic fraction was significantly reduced after enrichment using the ProteoExtract® Cytoskeleton Enrichment and Staining Kit, resulting in clear detection of insoluble, low-abundance actin-associated proteins (β -catenin).

Conclusions

Merck Millipore's ProteoExtract® Cytoskeleton Enrichment and Isolation Kit offers a convenient, efficient tool to purify cytoskeleton proteins with a gentle detergent buffer treatment for subsequent biochemical analysis. The ProteoExtract® Native Cytoskeleton Enrichment and Staining Kit preserves focal adhesion and cytoskeletal structure for imaging, and greatly reduces background emanating from soluble cytoplasmic proteins in the cell. Both kits will greatly enhance the ability to detect and analyze the low abundance actin-associated proteins which are typically masked in conventional methods.

References

- Chen CS et al. (2003). Biochem & Biophys Research Comm. 307(2):355-61.
- 2. Fri-94.
- 3. Bretscher A et al. (1994). J Cell Biol 126:821–825.
- 4. Dubreuil RR. (1991). BioEssays 13:219-226.
- 5. Matsudaira P. (1991). Trends Biochem Sci 16:87-92.
- 6. Matsudaira P. (1994). Semin Cell Biol 5:165-174.
- 7. Rao JY et al. (1990). Cancer Res 50:2215-2220.
- 8. Yamada KM, Geiger B. (1997). Curr Opin Cell Biol 9:76–85.
- 9. Burridge K et al. (1990). Cell Diff Dev 32:337–342.
- 10. Turner CE, Burridge K. (1991). Curr Opin Cell Biol 3:849-853.
- 11. Tristan C et al. (2011) Cell Signal 23: 317–323.

FEATURED PRODUCTS

Available from www.millipore.com

Description	Catalogue No.
ProteoExtract®	
Cytoskeleton Enrichment and Isolation Kit	17-10195
Native Cytoskeleton Enrichment and Staining Kit	17-10210

RELATED PRODUCTS

Available from www.merck4biosciences.com

Description	Catalogue No.
ProteoExtract*	
Subcellular Proteome Extraction Kit	539790
Subcellular Proteome Extraction Kit, Mini	539791
Cytosol/Mitochondria Fractionation Kit	QIA88
Complete Mammalian Proteome Extraction Kit	539779
Transmembrane Protein Extraction Kit	71772

Available from www.millipore.com

Description	Catalogue No.
Compartmental Protein Extraction Kit	2145
Actin Cytoskeleton and Focal Adhesion Staining kit	FAK100

ESGRO®-2i Medium: Inhibitor-Based Serum-free Medium for ES and iPS Cell Culture

Gabi Tremml, Ming Li and Vi Chu Merck Millipore

Introduction

Defined serum-free and feeder-free culture of mouse embryonic stem (mES) cells holds many advantages over the classical serum-containing feeder-dependent culture methods, ranging from decreased lot-to-lot variation to ease of culture. The discovery that the inhibition of differentiation inducing signals is critical for mES cell self renewal even in absence of the cytokine Leukemia Inhibitory Factor (LIF) led to a new definition of the ground state of ES cell self-renewal¹. Inhibitors that block MAPK/ Erk pathway, in combination with the glycogen synthase kinase 3 (GSK3) inhibitor, protect mES cells from differentiation-inducing signals, allowing for self-renewal in serum-free medium^{2,3}. However, mES cells maintain their LIF responsiveness^{1,4}. In this study, we explore the uses of the inhibitor-based, serum-free and feeder-free ESGRO®-2i medium from Merck Millipore.

Materials and Methods

Immunocytochemistry

For Oct-4 staining, we used mouse Oct-4 antibody (Santa Cruz) at a 1:100 dilution, and secondary donkey anti-mouse IgG-FITC (Merck Millipore, Cat. No. AP129F) antibody at a 1:500 dilution. For the SSEA-1 staining, we used mouse SSEA-1 antibody (Merck Millipore, Cat. No. MAB4301) at a 1:50 dilution, and secondary goat anti-mouse IgM-FITC (Jackson Laboratories) antibody at a 1:500 dilution.

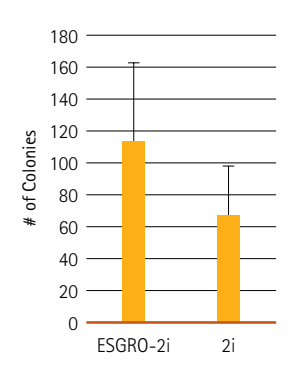
Low density clonal assay

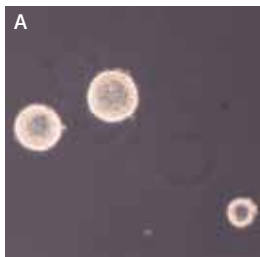
mES cells were expanded for 1-2 passages prior to low density clonal assay in ESGRO® Complete Plus Clonal Medium (Merck Millipore, Cat. No. SF001). Cells were split with Accutase™ reagent (Merck Millipore, Cat. No. SCR005),

washed twice with ESGRO® basal medium (Merck Millipore, Cat. No. SF002) and counted. 6-well plates were coated with 0.1% gelatin, and wells were seeded with 1000 cells/well in either ESGRO®-2i medium or in 2i medium (without LIF). After 5 days, colonies were counted.

Two-step RT-PCR with Amplifluor® primers:

mES cells and induced pluripotent stem cells (iPSCs) were cultured in a 6-well plate until confluence. Total RNA was extracted using the RNeasy® kit (QIAGEN). Samples were treated with RNase-free DNase prior to reverse transcription. cDNA was synthesized from total RNA with oligo(dT) and random hexamer primers mix provided with the iScript™ cDNA Synthesis Kit (Bio-Rad). 1 μg of total RNA was used in 20 µL of reaction. The reverse transcription reaction consisted of 25 °C for 5 minutes. 42 °C for 30 minutes, and 85 °C for 5 minutes. 2 µL of the reverse transcription reaction was used in PCR amplification. PCR reactions were carried out using STEMCCA™ Viral Gene Detection gPCR Multiplex Kits (Merck Millipore, Cat No. SCR581). Briefly, the multiplex qPCR reactions were carried out using TITANIUM™ Taq DNA polymerase (Clontech) with a final concentration of 6 mM MgCl_a and 300 µM dNTP. The PCR reaction consisted of an initial denaturation at 95 °C for 3 minutes followed by 45 cycles of 30 seconds at 95 °C and 30 seconds at 60 °C. Positive plasmid controls from the kits were used to generate template standard curves along with the unknown cDNA samples for later quantitative determination of the relative copy number of the samples. Expression levels of the viral Oct-4 and endogenous Nanog were normalized to the housekeeping GAPDH gene.





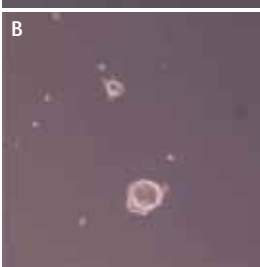


Figure 1. LIF responsiveness of 129SvEv mESCs. Emerging colonies from the low density clonal assay were counted and morphology documented. a) colonies in ESGRO®-2i which contains LIF, GSK3ß inhibitor, and Mek1/2 inhibitor. b) colonies in 2i which contains basal medium with GSK3ß inhibitor, and Mek1/2 inhibitor.

Results

During the development of ESGRO®-2i medium, we first compared 129SvEv mES cell propagation with a low density clonal plating assay in the presence of LIF (ESGRO®-2i) with propagation in the absence of LIF (2i). We found that the presence of LIF in the inhibitor medium led to better colony propagation and greatly enhanced the general health of ES colonies, confirming that pluripotent cells remained LIF-responsive (Figure 1).

After culturing 129SvEv mES cells for more than 10 passages in ESGRO®-2i medium, cells were injected into C57Bl6 host blastocysts. The resulting chimeras yielded germ line transmission (Table 1).



We analyzed the pool of injected mES cells for pluripotency markers, both by staining (Figure 2) and by quantitative RT-PCR (Figure 3) and found that relevant markers were expressed. Strikingly, one of the pluripotency markers, mouse nanog transcript (mNanog), underwent a 6-fold upregulation in mES cells in ESGRO®-2i medium when compared to mES cells cultured in parallel in serumcontaining medium on a feeder layer (Figure 3), suggesting that nanog upregulation is the mechanism by which ESGRO®-2i medium supports pluripotency. Moreover, ES cells could be derived from C57BI6 blastocysts in ESGRO®-2i medium at an efficiency of more than 10% (data not shown).

We then tested ESGRO®-2i medium for maintenance of pluripotency of induced pluripotent stem (iPS) cells. Currently, reprogramming is thought of as process by which cells revert through a primed state (pre-iPS cell) before they reach the naïve pluripotent state. These distinct states of pluripotency can be specified by culture conditions and are characterized by morphology, signaling pathway dependency, and epigenetic signatures. We hypothesized that ESGRO®-2i medium might provide the culture conditions to aid reversion of pre-iPS cells to the naïve state.

Foster Mother	# of Blastocysts	# of Cells Injected/ blastocyst	Live Births	Chimeras	% Chimerism	Germ Line Transmission
1	11	8–15 cells	3	1	90	Yes
2	10	8–15 cells	No Pregnancy	n/a	n/a	
3	10	8–15 cells	1	0	n/a	
4	10	8–15 cells	3	2	90, 60	Yes

Table 1. Chimera generation. 8–15 129SvEv agouti mESCs were injected into C57Bl6 blastocysts and a total of 41 blastocysts were transferred to four donor females. Chimerism was judged according to percentage of agouti coat color. Two 90% chimeras were backcrossed and germ line transmission was confirmed.

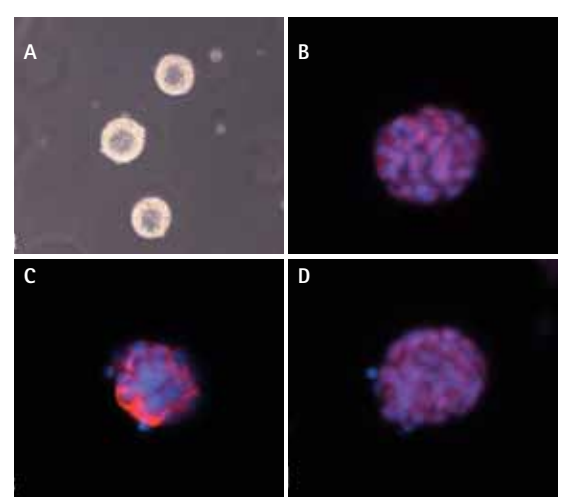


Figure 2. Prolonged pluripotent culture in ESGRO*-2i. 129SvEv mESCs were cultured for 10 or more passages. Pluripotency was assessed A) morphologically using bright field microscopy, B) with anti-Oct4 antibody staining, C) with anti-SSEA antibody staining, and d) with anti-Sox2 antibody staining.

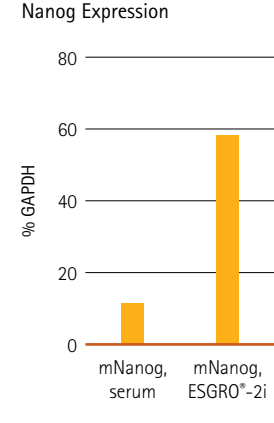


Figure 3. Nanog expression. ESGRO*-2i induces higher Nanog expression in 129SvEv mESCs cultured in ESGRO*-2i, compared to serum-containing culture.

To test this hypothesis, we generated several iPS cells with the STEMCCA™ polycistronic (OKSM) reprogramming lentiviral vector (Merck Millipore). Then, we expanded iPS cells both in ESGRO®-2i medium and in serum-containing medium on feeder layers. To measure the induction of pluripotency, we measured endogenous nanog expression as well as viral transgene expression represented by lentiviral Oct4 transcripts after 3-5 passages (early passage) and after 10 or more passages (late passage). We found that endogenous nanog up-regulation was concomitant with viral transgene down-regulation, after extended iPS cell culture in ESGRO®-2i medium. In contrast, neither upregulation of nanog nor down-regulation of viral Oct4 expression was observed in iPS cells cultured in serumcontaining conditions on feeder layers (Figure 4). This suggested that ESGRO®-2i medium aids in acquisition of naïve pluripotency and may be used to rescue partially reprogrammed iPS cells to a fully reprogrammed, naïve pluripotent state.

Moreover, we found two iPSC clones with morphological features of epiblast stem cells (EpiSCs), such as low clonogenicity, and low adherence in both culture conditions (data not shown). These clones had relatively high viral Oct4 and lower nanog transcript levels, suggesting a partially reprogrammed state. After prolonged culture in ESGRO*-2i medium but not after culture in serum-containing medium, we observed emerging adherent colonies with mES-cell-like morphological features, suggesting that ESGRO*-2i medium could provide a favorable culture condition for selection of naïve iPS colonies. Further studies are being performed to validate this observation.

Conclusion

Recently, LIF/2i medium was shown to provide a favorable environment for transitioning pre-iPS cells to naïve iPS cells⁵. This transition was accompanied by increased endogenous nanog expression while viral transgene expression was down-regulated, highlighting the role of nanog in facilitating acquisition of pluripotency⁶. This is consistent with our results, supporting evidence that maintenance of pluripotency in the defined ESGRO*-2i medium is mediated at least in part by nanog. In summary, we show that the defined serum-free and feeder-free ESGRO*-2i medium can be used for prolonged pluripotent mES cell derivation, maintenance and naïve iPSC culture.

References

- Ying Q-L. et al. The ground state of embryonic stem cell self-renewal. Nature. 2008; 452: 519–523.
- Chen S et al. Self-renewal of embryonic stem cells by a small molecule Proc Natl Acad Sci USA. 2006; 103: 17266–17271.
- Sato N. et al. Maintenance of pluripotency in human and mouse embryonic stem cells through activation of Wnt signaling by a pharmacological GSK-3-specific inhibitor. Nat Med. 2004; 10: 55–63
- Blair K Et al. The liberation of embryonic stem cells. PLoS Genet. 2011; 7(4): e1002019. doi:10.1371/journal. pgen.1002019
- Silva J et al. Promotion of Reprogramming to Ground State Pluripotency by Signal Inhibition. PLoS Biol. 2008; 6(10): e253. doi:10.1371/journal.pbio.0060253
- Theunissen, T.W. vanOosten A.L., Castelo-Branco G., Hall J., Smith A., and Silva J. (2011). Nanog overcomes reprogramming barriers and induces pluripotency in minimal conditions. Current Biology 21, 65–71.

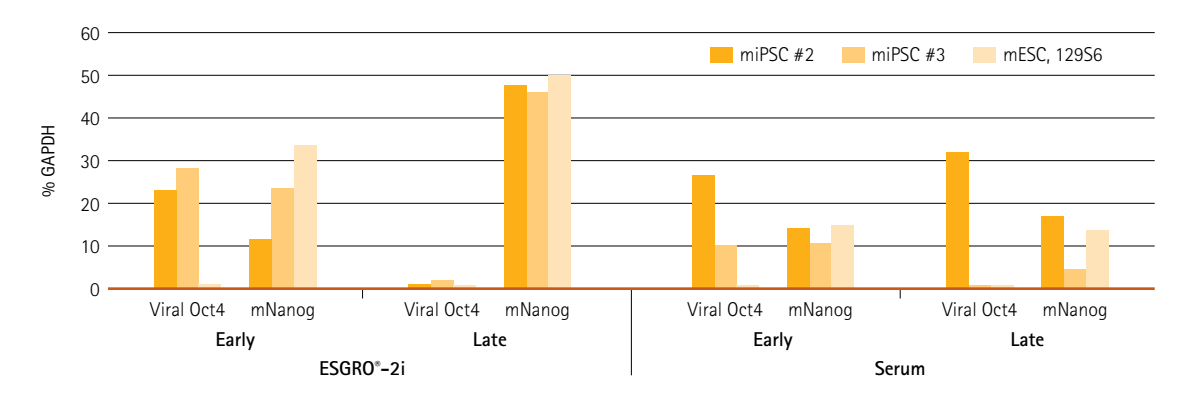


Figure 4. Nanog and Viral Oct4 expression in iPSCs. Viral Oct4 and mNanog transcript levels are shown in 129S6 mESCs at early passages (3–5), and at late passages (>10) in parallel cultures containing ESGRO®-2i medium or serum containing medium in the presence of feeder layers.

FEATURED PRODUCTS

Available from www.millipore.com

Description	Catalogue No.
ESGRO®-2i Medium	SF016-100; SF016-200
Donkey anti-mouse IgG-FITC	AP129F
Mouse SSEA-1 antibody	MAB4301
ESGRO® Complete Plus Clonal Medium	SF001-500P; SF001-100P
ESGRO® Basal Medium	SF002-500; SF002-100
Accutase™ Dissociation Solution	SCR005
Mouse STEMCCA™ Viral Gene Detection qPCR Multiplex Kit	SCR581
Mouse STEMCCA™ Constitutive Polycistronic (OKSM) Lentivirus Reprogramming Kit	SCR510

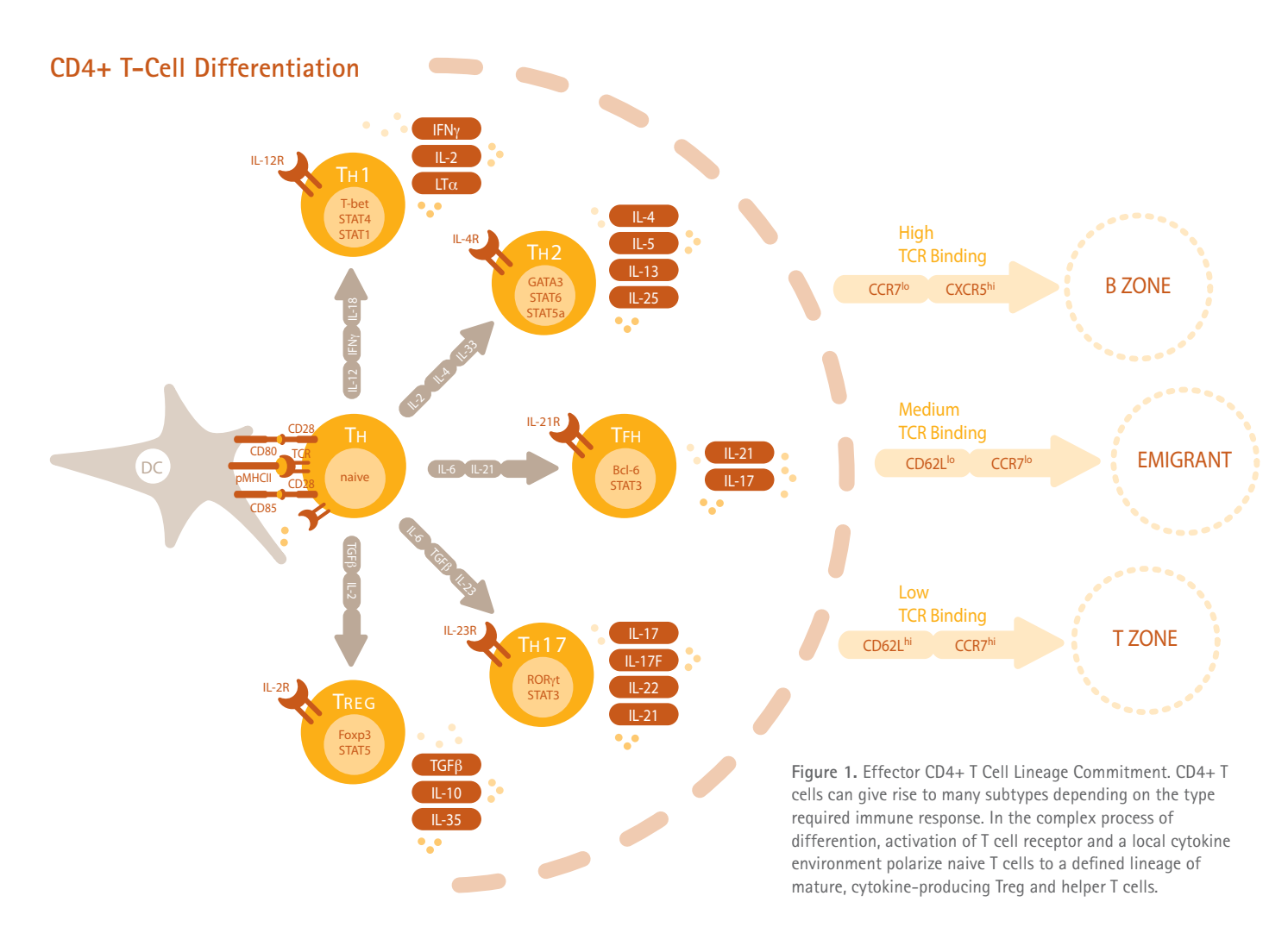
A Dual Platform Approach to Cytokine Analysis of Effector CD4+ T-Cells

Yuko Williams, Don Weldon, Wen-Rong Lie, Roberto Renteria, Jason Whalley and Matthew Hsu Merck Millipore

Abstract

The study of effector CD4+ T-cell differentiation is important for understanding inflammation and autoimmunity. Naive CD4+ T cells can give rise to many subtypes depending on the nature of the immune response. Each subtype expresses a signature cytokine or a transcription factor that directs the type of immune response needed. *In vitro*- generated effector T cells are useful for studying mature T-cell differentiation, cytokine analysis and functional characterization. We have developed standardized primary culture systems optimized for differentiating naive CD4+ cells into four major effector cell

lineages (Helper T (Th) 1, Th2, Th17 and regulatory T (Treg)). Each culture system contained a CD3 antibody-coated culture plate, media, and cocktail of activating factors. Using multiplexed immunoassays, the differentiated T cells were shown to secrete the signature cytokines. Intracellular cytokines and transcription factor expression were also measured using benchtop flow cytometry. Effector CD4+ cells generated by this optimized culture system produced lineage-specific or signature cytokines, indicating that they are effective tools for functional characterization of T cell subtypes.



Materials and Methods

Generation of cytokine-producing effector T cells

Mouse CD4+ splenocytes were differentiated to one of four distinct lineages through a process of activation, expansion, and re-stimulation (Figure 2). The cells were activated by culturing on anti-CD3-coated plates with the single addition of a combination of growth factors and antibodies in precise amounts to begin the differentiation process. They were further expanded, then re-stimulated at day 4 and 6. After day 6, the differentiated cells secrete their signature cytokines and can be assayed.

Measurement of signature cytokines using multiplexed immunoassays

MILLIPLEX® MAP Mouse Cytokine /Chemokine Magnetic Bead Panel I (Cat No. MCYTOMAG-70K) was used to measure the secreted cytokine concentrations in cultured mouse Th1 and Th17 cells. Based on Luminex® technology, this magnetic bead-based multiplex immunoassay kit can simultaneously detect up to 32 mouse cytokines and chemokines, including IFN , TNF α (Th1 cytokines) and IL-17 (a Th17 cytokine) and it requires only 25 μL of assay standard or culture supernatant sample per well. In this study, the assay standard curves and culture supernatant samples (± Brefeldin A) were evaluated in duplicate. The culture supernatants were diluted 1:10 in Assay Buffer for analysis. Automation of wash steps for the 96-well microplate assay was done with the ELx405 Microplate Washer. Data were acquired and analyzed using the Luminex 200™ System (Cat No. 40-013) MILLIPLEX® Analyzer with MILLIPLEX® Analyst Software.

Characterization of T cell subtypes using benchtop flow cytometry

Naive CD4+ cells and differentiated cells were first stained with viability dye to identify the dead cells. This was followed by staining for signature intracellular cytokines IL-4, IL-17, interferon gamma (IFNγ), and FoxP3 along with the surface marker CD4 by using the FlowCellect™ Mouse Th Intracellular Cytokine Kits. Quadrants were set based on unstained cell samples. Data were acquired and analyzed using an easyCyte™ benchtop flow cytometer and guavaSoft™ software.

Results

In order to quantitatively measure the amount of cytokines secreted by the differentiated effector T cells, a multiplexed mouse cytokine magnetic bead panel was used to assay the media from the cultured cells. Interferon gamma (IFN γ), the signature cytokine for Th1 cells, and IL-17, the signature cytokine for Th17 cells, were quantified on both Th1 and Th17 differentiated cells to demonstrate assay specificity. The Th1 differentiated cell culture showed secretion of IFN γ into the medium; however, it did not show IL-17. The Th17 medium was positive for IL-17 but not IFN γ . Therefore, we concluded that each of the differentiated cell types specifically secreted its signature cytokine.

The quantitative measure of the amount of secreted cytokine tells half of the story. Although measuring total soluble secreted cytokine showed that each cell type was definitely producing signature cytokines, we could not tell which individual cells were producing the cytokine or at

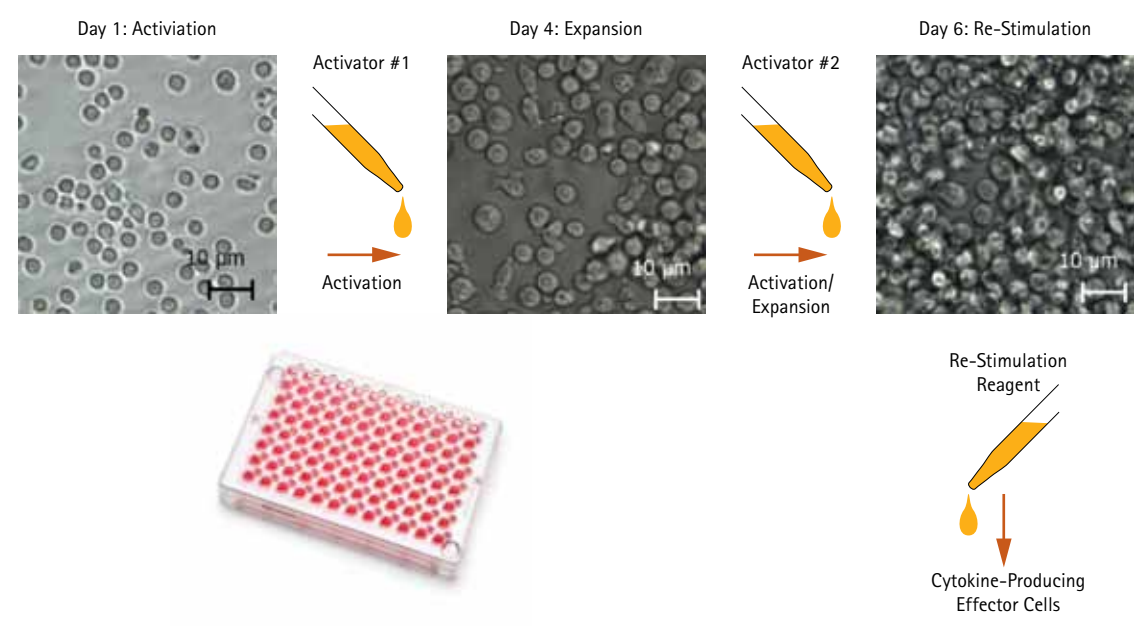


Figure 2. Six-day differentiation protocol. Day 1: Activation. Culture CD4+ cells with growth factors, neutralizing antibodies, and the T cell receptor costimulator on an anti-CD3 coated 96-well plate for 3 days. Day 4: Expansion. Expand activated/developing CD4+ cells in a larger tissue culture plate. Day 6: Re-Stimulation. Differentiated effector cells are re-stimulated with mitogens to induce lineage-specific cytokine production. Note that this step is not necessary for Treg differentiation.

what level. For example, it was possible that 5% of the cells were secreting large amounts of cytokine to give the total amount detected using the MILLIPLEX® assay. Alternatively, it was possible that all of the cells are secreting low levels of cytokine. We could not distinguish these two possibilities from the MILLIPLEX® assay alone.

By blocking the secretion of cytokine using Brefeldin A (BFA, a protein transport inhibitor) we trapped the cytokine inside cells. Once cytokines were blocked from being secreted, we identified which cells were producing the cytokine and determined the level of cytokine production in each cell (Figure 3A and 3B). Benchtop flow cytometry enabled the analysis of cytokine production at a single-cell level, and showed that production of intracellular cytokines correlated with results from the MILLIPLEX® assay. BFA increased cytokine expression levels within individual cells but not the percentages of positive populations (F/C). This added level of information completed our picture of signature cytokine production within differentiated CD4+ cells.

Due to high turnover rates for the secreted cytokines, the cells not treated with BFA showed varying expression levels of signature cytokines. Once cells were treated with BFA, higher percentages of cytokine-expressing cells were observed.

Four T cell subtypes were analyzed using easyCyte™ benchtop flow cytometry to measure levels of characteristic intracellular cytokines. As shown in Figure 4, Th1, Th2, Th17 and Treg differentiated cells expressed enriched levels of signature cytokines IFNγ, IL-4, IL-17, and FoxP3, respectively, compared to naïve CD4+ T cells.

Conclusion

Differentiated effector CD4+ cells can be useful for determining the effects of compounds or treatments *in vitro* when followed by quantitative analysis of both signature as well as related cytokines The standardized primary culture systems used in this study provide an optimized method for differentiating CD4+ effector T cells with consistent results, and are a promising, new tool for functional characterization of inflammation/immune response pathways.

As shown in this study, a dual approach for quantifying cytokine expression can provide an accurate, rich assessment of T-cell differentiation. MILLIPLEX® mouse cytokine/chemokine magnetic bead panels provide a fast, quantitative method for determining cytokine levels secreted by differentiated effector T cells, requiring only minimal sample volume. These data are complemented by flow cytometry analysis, which shows which cells are secreting the cytokines and at what levels. Using a viability dye eliminated false positives, enabling more accurate analysis of these heterogeneous cell populations.

A MILLIPLEX® Multiplexed Immunoassay

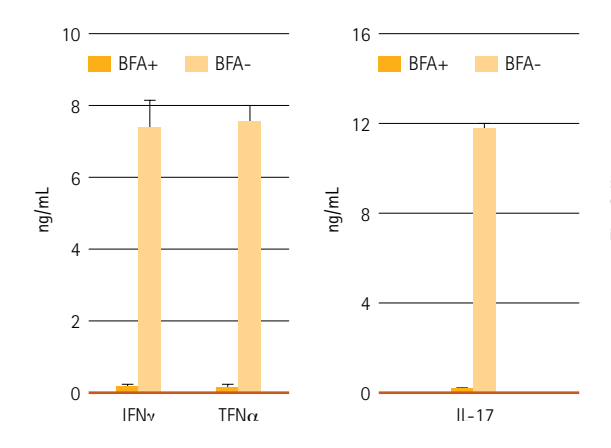
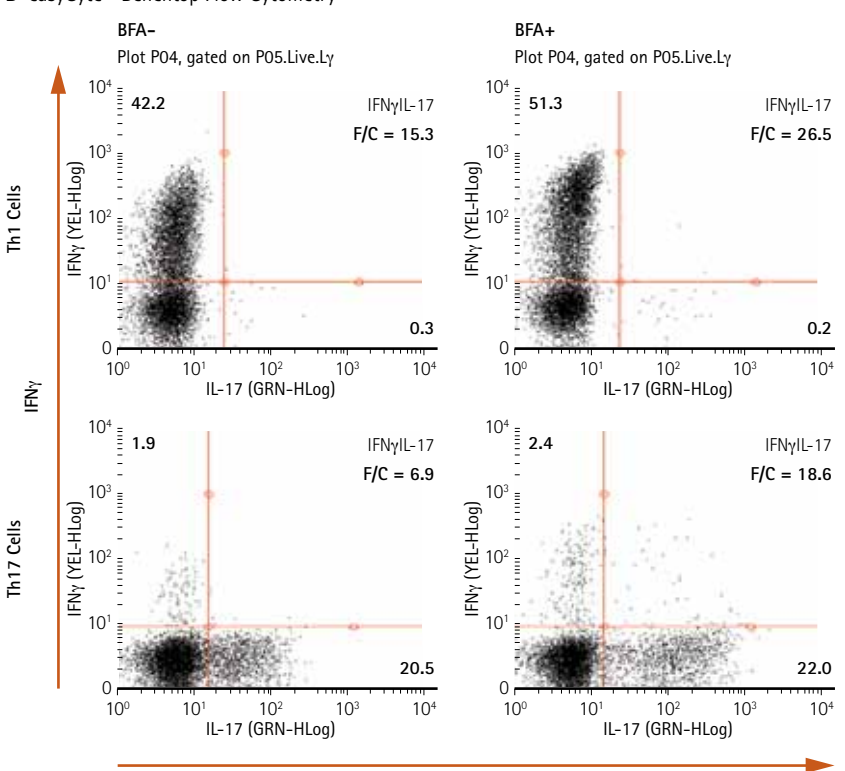


Figure 3. Two analytical methods show that Th1 and Th17 cells generated by in vitro differentiation secrete signature cytokines. A. Analysis of cytokine secretion in supernatant media from Th1 and Th17 differentiated cell cultures using MILLIPLEX® multiplexed immunoassays. Error bars represent standard error of the mean. B. Intracellular cytokine analysis using easyCyte™ benchtop flow cytometry. BFA=Brefeldin A, Fold changes (F/C) in cytokine expression were calculated as follows: F/C = Mean Fluorescence Intensity (MFI) of cytokine-positive population/MFI of cytokine-negative population.

B easyCyte[™] Benchtop Flow Cytometry



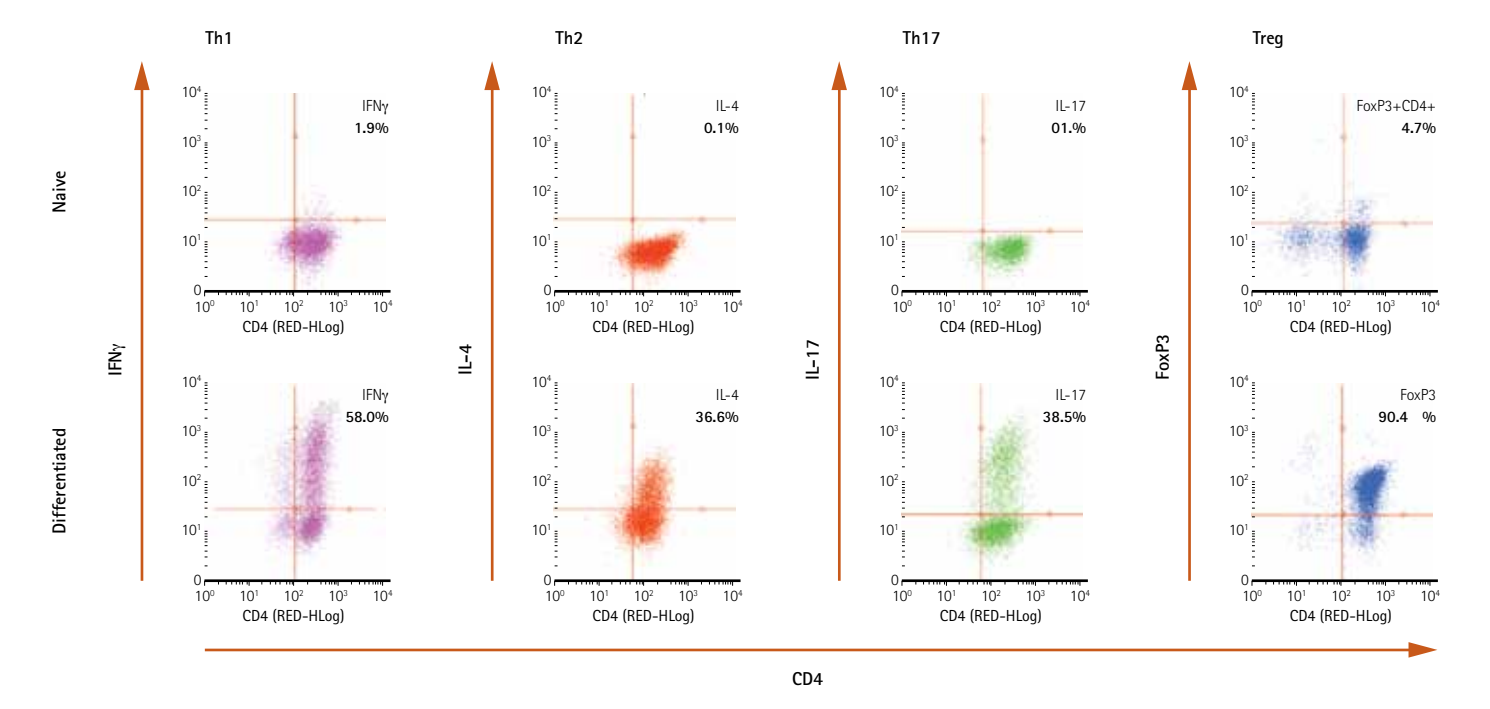


Figure 4. Intracellular cytokine staining of Th1, Th2, Th17 and Treg differentiated cells. Mouse naive CD4+ cells were differentiated for 6 days under polarized culture conditions using FlowCellect™ Differentiation Tool Kits. On day 6 of culture, Th1, Th2 and Th17 were re-stimulated with mitogens 5 hours prior to harvest. Naive CD4+ cells (top row) and differentiated cells (bottom row) were analyzed using easyCyte™ benchtop flow cytometry.

Description	Catalogue No.
lowCellect™	
Mouse TH1 Intracellular Cytokine Kit	FCIM025123
Mouse TH2 Intracellular Cytokine Kit	FCIM025124
Mouse TH17 Intracellular Cytokine Kit	FCIM025125
Mouse TH1/TH2 Intracellular Cytokine Kit	FCIM025137
Mouse TH1/TH17 Intracellular Cytokine Kit	FCIM025138
Mouse Viable Treg Characterization Kit	FCIM025168
Mouse Breg Identification Kit	FCIM025154

MCYTOMAG-70K

17-10210

NOW AVAILABLE

Mouse Cytokine/Chemokine Magnetic Bead Panel

Mouse Cytokine/Chemokine Magnetic Bead Panel II

FEATURED PRODUCTS

Available from www.millipore.com

Description	Catalogue No.
FlowCellect™	
Mouse TH1 Differentiation Tool Kit	FCIM025161
Mouse TH2 Differentiation Tool Kit	FCIM025162
Mouse TH17 Differentiation Tool Kit	FCIM025163
Mouse Treg Differentiation Tool Kit	FCIM025166

Rapid Counting of Somatic Cells in Dairy Milk Using the Scepter[™] 2.0 Cell Counter, Following Spin-Wash Sample Preparation

Amedeo Cappione, Ph.D. and Janet Smith Merck Millipore

Introduction

Mastitis is an inflammatory change in the mammary gland characterized by pathological changes in mammary tissue. This potentially fatal infection is the most common and most costly disease facing the United States dairy industry¹. Milk from sick cows exhibits increased somatic cell counts (SCC) due to the release of white blood cells into the gland to combat infection. Samples displaying SCC ≤200,000 cells/ mL are considered healthy, values ≥300,000 cells/mL are indicative of early stages of infection (subclinical mastitis), and counts ≥750,000 cells/mL denote full-blown mastitis. Given that subclinical cases present the greatest cost burden due to a lack of physical indications, research efforts designed at targeting rapid detection of elevated SCC counts as well as therapeutic interventions are critical to sustaining the dairy market.

Milk is an emulsion of fat globules in a water-based fluid. Milk fat globules possess a number of attributes which severely hinder accurate somatic cell counting.

Characteristics of Milk Fat Globules Hindering Somatic Cell Counting:

- Significantly more abundant than cells. Depending on the sample, this difference can be on the order of 5000X.
- Stick to cells, forming aggregates that must be dispersed prior to sized-based detection.
- Diameter range: 0.1–20 μm; globule size overlaps with the average somatic cell diameter (8.5–10 μm)
- Content varies significantly, both cow-to-cow and day-to-day



Most current methodologies for measuring SCC in milk involve the use of cell-specific fluorescent dyes to analyze samples using flow cytometry and microscopy.

The Scepter™ handheld, automated cell counter provides a rapid, reliable alternative to traditional SCC analysis. The device combines the ease of automated instrumentation and the accuracy of the Coulter principle of impedance-based particle detection in an affordable, handheld format.

The Scepter™ cell counter uses a combination of analog and digital hardware for sensing, signal processing, data storage, and graphical display. The precision-made, consumable polymer sensor has a laser-drilled aperture in its cell sensing zone that enables the instrument to use the Coulter principle to discriminate cell diameter and volume at submicron and subpicoliter resolution, respectively. The spin-wash protocol, when used in conjunction with the Scepter™ cell counter and 40 µm aperture sensor, enables rapid, precise somatic cell counting with results comparable to fluorescence-based platforms.

Materials and Methods

Samples

Fresh milk samples (40–50 mL) were routinely acquired from a local dairy farm, Dunajski Dairy (Peabody, MA). Samples were stored at 4 °C and used within 48 hours before disposal. Prolonged storage resulted in appreciable changes to both the fat and cell content.

Spin-wash protocol for dairy milk sample preparation

Upon standing for 12 to 24 hours, fresh milk separates into a high-fat "cream" layer and a larger, low-fat milk layer. The fat globules rise to the top because fat is less dense than water. Separation can also be accomplished rapidly through centrifugation. The protocol is as follows:

- 1. Allow milk and phosphate-buffered saline (PBS) to come to room temperature.
- 2. Add 500 μL PBS to 500 μL milk in a 1.5 mL microfuge tube.
- 3. Mix quickly by vortexing.
- 4. Centrifuge at 1000 g for 2 minutes in a tabletop centrifuge.
- 5. Remove upper cream layer using a cotton swab, pour off remaining skim layer.
 - a. The cream layer is very viscous and will stick to the sides of the tube. Attempt to remove as much as possible by gently swirling the cotton swab.
 - b. A white pellet containing cells and fat should be visible at the bottom of the tube.
- 6. Add 1 mL PBS to the tube. Do not resuspend pellet.
- 7. Repeat steps 4–6 twice.
 - a. Certain samples may require additional spin cycles to achieve sufficient removal of fat for cell detection.
- 8. After the final spin, resuspend the cell pellet in 500 μ L PBS by gently pipetting up and down.
- 9. Acquire cell concentration and cell size data using a Scepter™ cell counter equipped with a 40 μm aperture sensor
 - a. The 40 μ m sensor has an upper detection limit of 1.5 x 10 6 cells/mL. For this reason, certain samples may need to be further diluted for accurate counting.

SSC testing on a guava easyCyte[™] flow cytometer

Following spin-wash, aliquots of each sample were mixed with ViaCount® reagent (Merck Millipore). The reagent contains a cell-permeant nuclear dye that preferentially labels cells.

Stained samples were analyzed on the guava easyCyte™ flow cytometer (Merck Millipore). For each sample, 10,000 total events were acquired.

External SCC testing

For each milk sample, SCCs were verified by Agri-Mark Dairy Cooperative (Lawrence, MA). Samples were tested using a Fossomatic™ cell counter (Foss, Denmark), a fluorescence-based flow cytometry platform.

Percent recovery studies

Jurkat cells were labeled using CellTracker® Green CFMDA (5-chloromethylfluorescein diacetate, Life Technologies). Dye was resuspended in DMSO to 10 mM. Cells were labeled by incubating 1 e6/mL in fresh culture media at 37 °C for 30 min with 1:1000 dilution of dye. Cells were washed 2X with PBS prior to use. Cells were added to milk samples at known concentrations. Following a short equilibration time, milk samples were processed and analyzed using the guava easyCyte™ flow cytometer.

Results

To determine the effectiveness of fat globule removal by the spin-wash method, samples were processed as follows: (1) 1:1 dilution in PBS, (2) One spin-wash, and (3) Three spin-washes. Processed samples were analyzed with the Scepter™ cell counter using 40 µm sensors. The results presented in Figure 1 are from a sample with high SCC. The top row displays diameter histogram plots acquired on the Scepter™ cell counter. Initial attempts at Scepter™ analyses of whole milk proved unsuccessful; over half the samples resulted in sensor failure due to either "Lost Start" errors (due to air bubbles or insufficiently submerged sensors) or blocked apertures. Samples™ that could be read displayed concentration values that greatly overestimated true SCC values due to fat globule interference. For samples treated with three spin-wash cycles, the 40 µm sensor showed a clear, distinguishable peak corresponding to the somatic cell fraction. While three spin-wash cycles were sufficient to permit visualization of somatic cells in most samples, additional wash steps were required for samples with extremely high fat content.

Somatic cell detection was also confirmed through fluorescent labeling using ViaCount® reagent and the guava easyCyte™ cytometer. The middle row of histograms shows a distinct peak of fluorescently labeled cells (red) even in the unwashed fraction. As 10,000 total events were collected for each sample, the change in relative size of the fat (green) and cell (red) peaks with increased wash cycles confirms the removal of fat globules. In the bottom row, Foward Scatter (FSC) vs. Side Scatter (SSC) dot plots revealed cells (black) being released from fat aggregates as well as the relative decrease in number and size of fat globules (red) with successive washes.

The concentration of somatic cells in milk samples can vary greatly depending on diet, time relative to pregnancy, and overall health status. To test the performance range of the spin-wash method, we assessed a number of samples from both healthy cows and those presenting with mastitis. The spin-wash method was equally successful at enriching for the somatic cell fraction across a wide range of somatic cell counts. Representative examples of low (healthy), medium, and high SCC (mastitis) milk samples are displayed in Figure 2. For Scepter[™]-derived histograms, a distinct peak was seen for all three sample types. In each case, the mean diameter of this peak was consistent with the reported size range for bovine somatic cells. Cell counts were confirmed by flow cytometry. Results presented in the dot plots showed a significant increase in the frequency of detected cells (black) in high SCC samples as compared to low SCC samples. These increases paralleled the larger peak sizes demonstrated by the Scepter™ histograms.

Twelve samples were processed and analyzed (Figure 3). Overall, the Scepter[™]-derived SCC showed good agreement with values acquired using flow cytometry (Figure 3A). However, in nearly all cases, Scepter™ cell counts were slightly higher than flow cytometry values; this difference may be due to greater distinction of cells from fat afforded by fluorescent labeling for flow cytometry. The plotted values represent the mean of 3 replicates; both platforms showed high reproducibility in sampling results with average percent coefficient of variation (%CV) of 4.5 (Scepter™ cell counter) and 5.0 (guava easyCyte™ flow cytometer). Although slightly lower in all cases, results from both systems were also consistent with those determined externally (Agri-Mark; Figure 3B) on whole milk, a result which may be due to cell loss during the washing protocol.

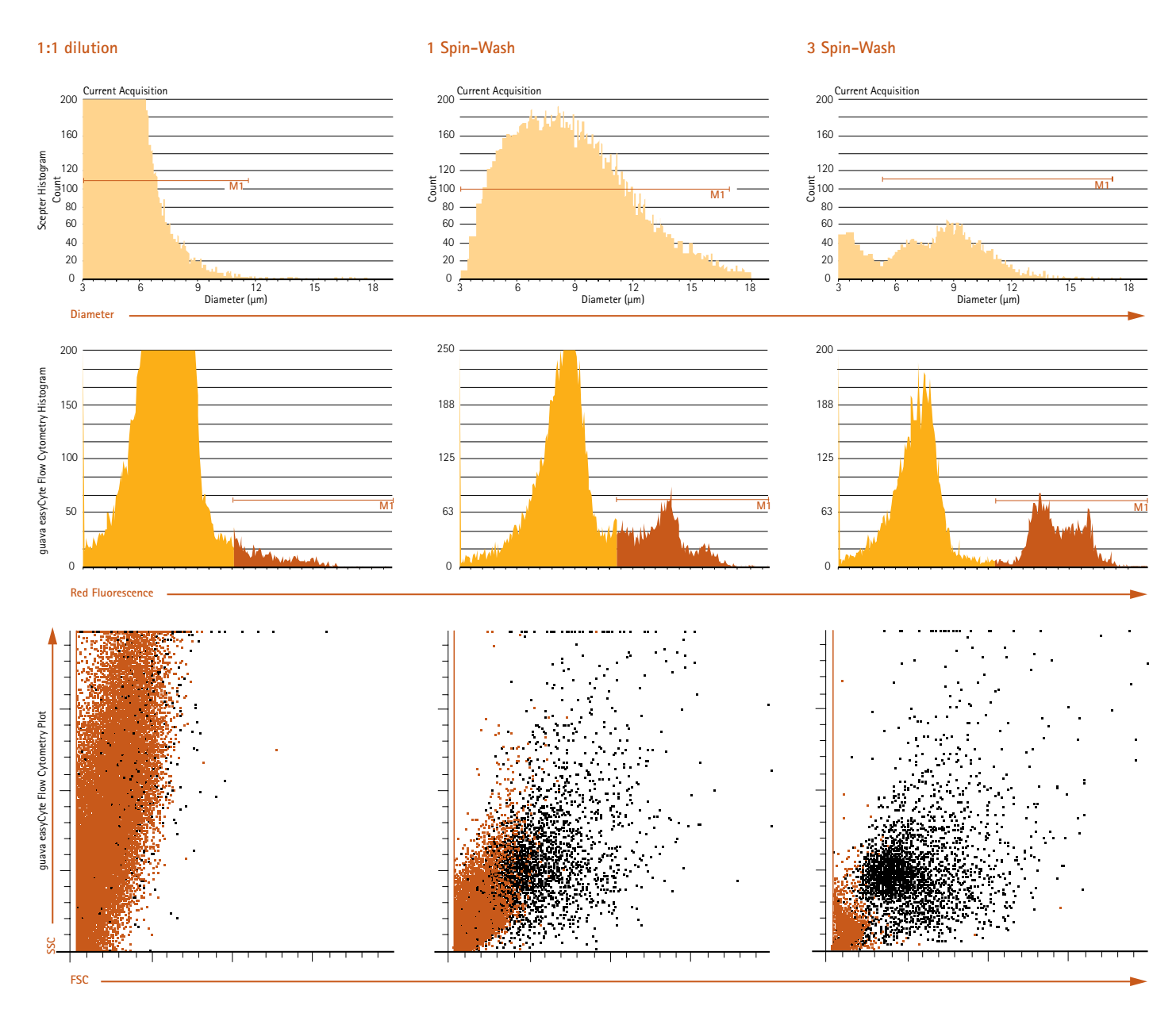


Figure 1. Spin-wash treatment effectively removes fat globules from dairy milk samples.

To quantify this possible cell loss, fluorescently labeled Jurkat cells were added to milk samples at known concentrations. Samples were subjected to multiple rounds of spin-washes and analyzed by flow cytometry to determine the degree of cell loss (below. While we observed a slightly greater cell loss with decreasing starting number, losses were no greater than 15% in any sample after three rounds of washes. These findings help substantiate the difference in SCC values calculated using the Scepter™ or guava easyCyte™ platforms and external testing.

	%	Cel	ΙR	ec	٥١	/er	V
--	---	-----	----	----	----	-----	---

	70 CCII NCCOVCI y		
Jurkat Cell Input	1-spin	2-spin	3-spin
50000	95.6	91.3	85.9
200000	97.9	92.7	88.7
500000	97.3	93.7	90.8
1000000	97.7	94.1	90.1
3000000	98.8	94.8	91.5

Conclusion

The Scepter™ cell counter offers the accuracy of impedance -based particle detection in an intuitive, as well as affordable, handheld format. The new 40 µm aperture sensor offers expanded sensitivity for discrimination of smaller cells and particles. This platform, when used in conjunction with the Spin-wash protocol, provides a quick and reliable method for accurate somatic cell counting in milk samples.

 Viguier, C., Arora, S., Gilmartin, N., Welbeck, K., and O'Kennedy, R. (2009) Mastitis Detection: Current Trends and Future Perspectives. Trends in Biotechnology. 27(8):486-93.

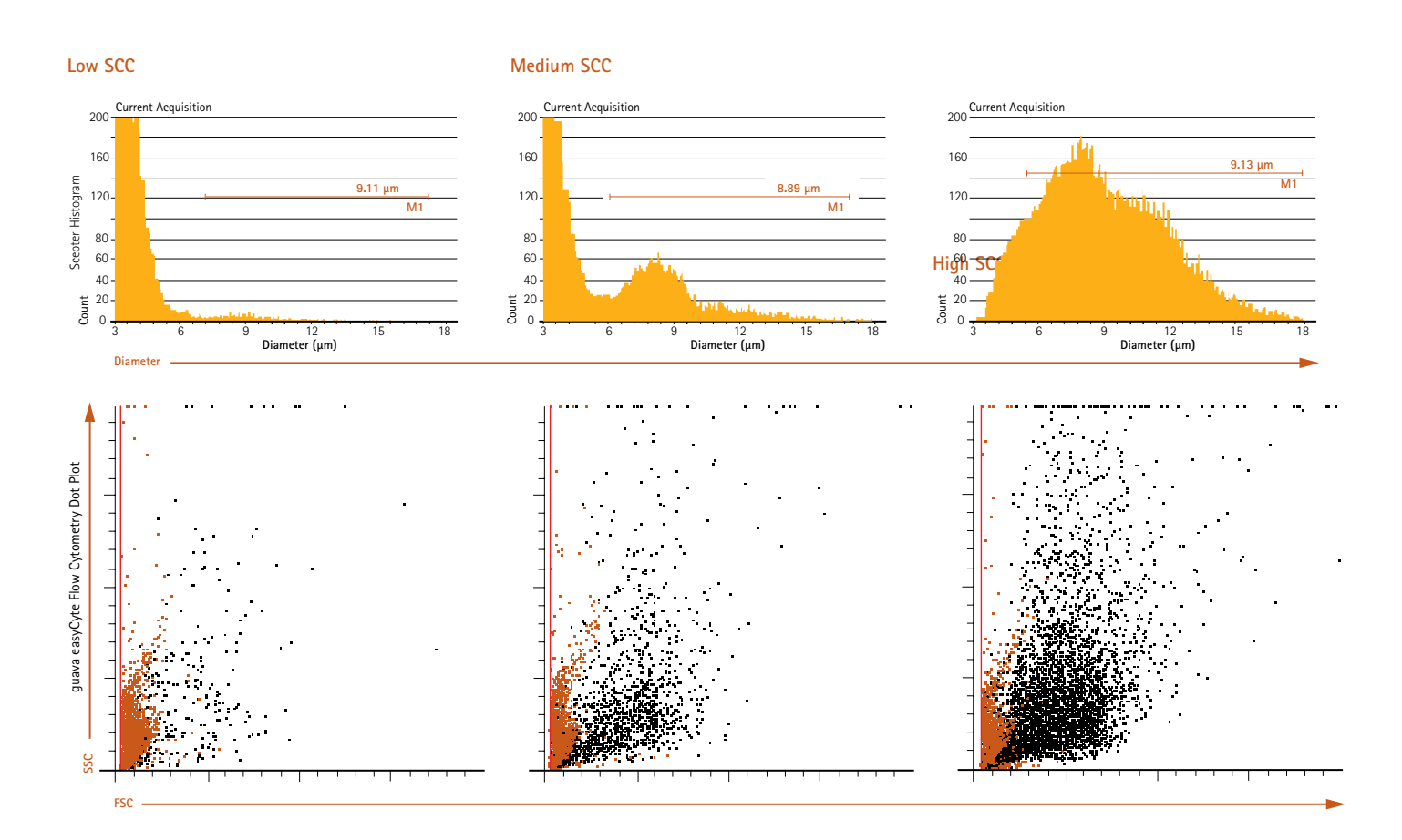


Figure 2. Scepter™ cell counting and guava easyCyte™ flow cytometry provide interpretable SCC data for dairy milk samples containing low, medium and high numbers of somatic cells.

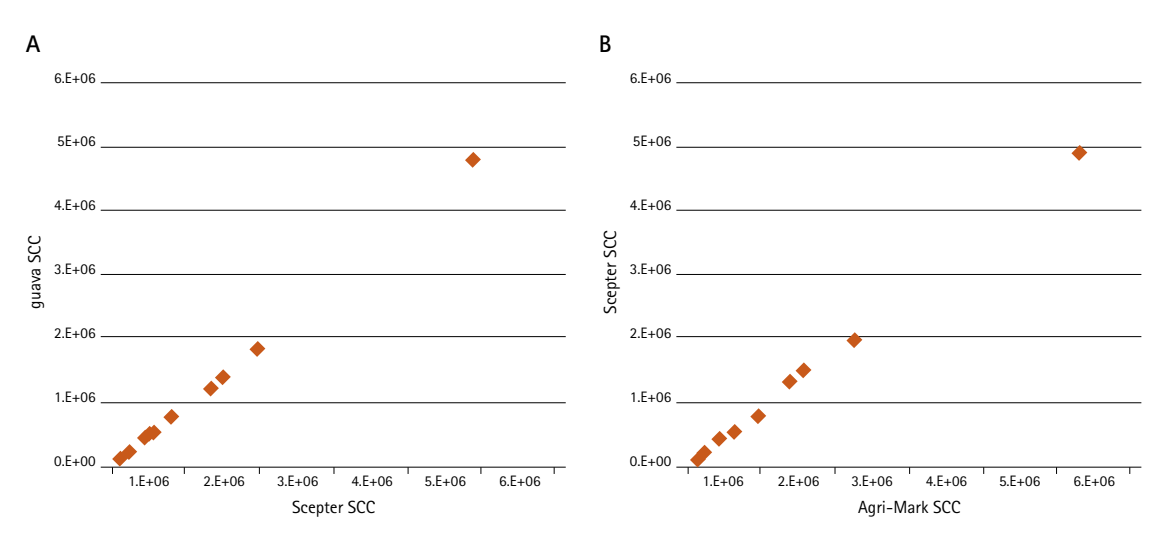


Table 3. Highly correlated SCC data between three cell counting platforms:
(A) guava easyCyte™ values are derived from the number of fluorescently labeled cells following ViaCount® staining.
(B) Agri-Mark is an external SCC testing facility.

FEATURED PRODUCTS

Available from www.millipore.com

Scepter™ 2.0 Cell Counter

Description	Qty	Catalogue No.
Scepter™ 2.0 Handheld Automated Cell Counter		
with 40 μm Scepter™ Sensors (50 Pack)	1	PHCC20040
with 60 μm Scepter™ Sensors (50 Pack)	1	PHCC20060
Includes:		
Scepter™ Cell Counter	1	
Downloadable Scepter™ Software	1	_
0-Rings	2	_
Scepter™ Test Beads	1	PHCCBEADS
Scepter™ USB Cable	1	PHCCCABLE
cepter™ Sensors, 60 μm	50	PHCC60050
	500	PHCC60500
Scepter™ Sensors, 40 μm	50	PHCC40050
	500	PHCC40500
Universal Power Adapter	1	PHCCPOWER
Scepter™ 0-Ring Kit, includes 2 0-rings and 1 filter cover	1	PHCCOCLIP

Guava easyCyte™ Benchtop Flow Cytometers

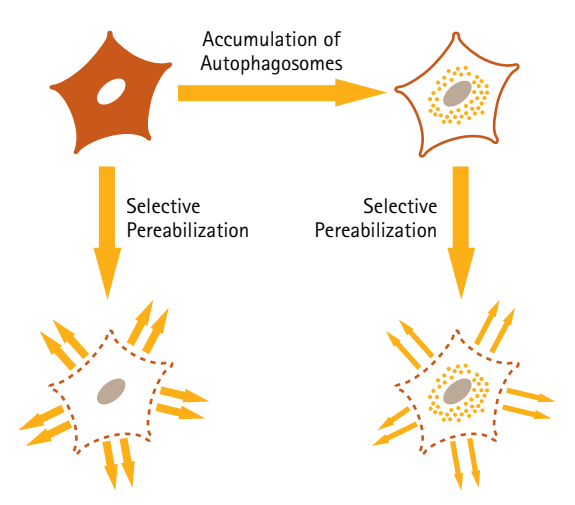
Description	Qty	Catalogue No.
High-Throughput Sampling Instruments		
guava easyCyte™ 8HT Base System	1	0500-4008
guava easyCyte™ 6HT/2L Base System	1	0500-4007
guava easyCyte™ 5HT Base System	1	0500-4005
PCA-96 Base System	1	0100-8710
Single Sampling Instruments		
easyCyte™ 5 Base System	1	0500-5005
easyCyte™ 6-2L Base System	1	0500-5007
easyCyte™ 8 Base System	1	0500-5008

Exciting New Products for Cell Biology Research

FlowCellect™ LC3-GFP Reporter Autophagy Assay Kits

Upon induction of autophagy, LC3 (the mammalian homolog of the small protein Atg8) is conjugated to phosphatidylethanolamine and recruited to the autophagosome membrane, targeting the autophagosome for fusion with the lysosome. The FlowCellect™ LC3-GFP Reporter Autophagy Assay Kit provides a quantitative solution for studying autophagy and measuring potency of autophagy inducers using flow cytometry. The kit has three unique features:

- Included selective permeabilization solution enables measurement and visualization of LC3-GFP translocation by extracting the soluble cytosolic LC3-GFP while protecting LC3-GFP that has been sequestered into the autophagosome.
- Monomeric GFP reporter minimizes dimer formation and aggregation, facilitating translocation and resulting in more accurate flow cytometry analysis.



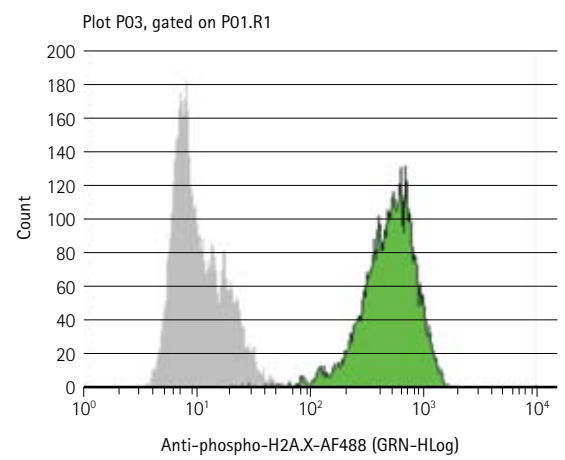
Selective permeabilization helps discriminate cytosolic from autophagic LC3 Separation of GFP-cytosolic LC3-I from autophagosome-associated GFP-LC3-II is achieved by disruption of the plasma membrane by using a proprietary, autophagy-enabling solution. This selective permeabilization releases cytosolic LC3 by flushing it away during washing steps. LC3-II, trapped in the autophagosome, remains intact, and fluorescence can be measured.

 Since autophagy is a constitutive cellular degradation process, the use of lysosomal degradation inhibitors prevents the degradation of LC3 fusion protein, prolonging the assay signal and enabling its quantification by flow cytometry.

FlowCellect™ Histone H2A.X Phosphorylation Assay Kit

Phosphorylation of the histone variant H2A.X is a rapid and sensitive response to double strand DNA breaks, induced by UV radiation, chemotherapeutic agents, or other cellular stresses. Phospho-H2A.X then helps recruit other damage reponse proteins. This assay kit includes a directly conjugated antibody, Anti-phospho-Histone H2A.X (Ser139)-Alexa Fluor® 488, and is a sensitive, valuable tool for measuring the extent of DNA damage in a given cell population.

Like all FlowCellect™ kits, these new assays are thoroughly validated and optimized to yield accurate flow cytometry data when used with easyCyte™ benchtop flow cytometers as well as other flow cytometry instruments.



Etoposide (100 µM) induces DNA damage in HeLa cells, as seen by staining with the FlowCellect™ Histone H2A.X Phosphorylation Assay Kit. A noticeable shift to the right is indicated for the treated sample (green). Untreated HeLa cells (grey) were also stained and results are shown overlaid.

FEATURED PRODUCTS

Available from www.millipore.com

Description	Qty	Catalogue No.
FlowCellect™ Histone H2A.X Phosphorylation Assay Kit	100 Tests	FCCS100182
FlowCellect™ LC3-GFP Reporter Autophagy Assay Kit (CH0)	100 Tests	FCCH100170
FlowCellect™ LC3-GFP Reporter Autophagy Assay Kit (U20S)	100 Tests	FCCH100181

Scepter[™] 2.0 Monitor Immune Cell Types in Seconds

Discover the fastest, easiest way to count and discriminate subsets of immune cells with the industry's finest instrument for effortless cell analysis.

Scepter^M, the first handheld automated cell counter, brought portable and precise cell counting to the palm of your hand. Scepter^M 2.0 expands your ability to precisely count particles as small as 3 μ m, so you can analyze red blood cells, lymphocytes, monocytes and T-celll activation.



Cellutions:

The Newsletter for Cell Biology Researchers

To subscribe to our quarterly Cellutions newsletter and read about the latest research, new products, and innovative protocols for revolutionizing cell culture and analysis, visit www.millipore.com/cellutions.

To Place an Order or Receive Technical Assistance

In Europe, please call Customer Service:

France: 0825 045 645 Germany: 01805 045 645 Italy: 848 845 645

Spain: 901 516 645 Option 1 Switzerland: 0848 645 645 United Kingdom: 0870 900 4645 For other countries across Europe, please call: +44 (0) 115 943 0840

Or visit www.merckmillipore.com/offices

For Technical Service visit:

www.merckmillipore.com/techservice



www.merckmillipore.com

Merck Millipore and the M mark are trademarks of Merck KGaA, Darmstadt, Germany. ProteoExtract, WideScreen, and BeadPlex are registered trademarks of Merck KGaA, Darmstadt, Germany. ESGRO, MILLIPLEX, Amplifluor, Viacount and Milli-Q are registered trademarks of Millipore Corporation. STEMCCA, Scepter, FlowCellect, guavaSoft, Accutase and easyCyte are trademarks of Millipore Corporation. Alexa Fluor and CellTracker are registered trademarks of Molecular Probes. iScript is a trademark of Bio-Rad, Inc. Fossomatic is a trademark of Foss Electric, Ltd. TITANIUM is a trademark of Clontech. Luminex, XPONENT, and xMAP are registered trademarks of Luminex Corporation. Luminex 200 is a trademark of Luminex Corporation. Lit No. PR3774ENEU Job No. LS SBU-11-05048 Printed in the USA 10/2011 @2011 Millipore Corporation, Billerica, MA 01821 U.S.A. All rights reserved.

Branching Out in Stem Cell Research

Partner with Merck Millipore to expand the scope and power of your stem cell research. Our stem cell scientists work with our customers to stay on the cutting edge of technology and bring you the best of what's new.

Visit our stem cell site at www.millipore.com/stemcells to stay up to date.

Get Connected!

Join Merck Millipore Bioscience on your favorite social media outlet for the latest updates, news, products, innovations, and contests!



facebook.com/MerckMilliporeBioscience



twitter.com/Merck4Bio